Title

Blimp-1–dependent and –independent natural antibody production by B-1 and B-1–derived plasma cells

Journal

Journal of Experimental Medicine, 214(9)

ISSN

0022-1007

Authors

Savage, Hannah P
Yenson, Vanessa M
Sawhney, Sanjam S
et al.

Publication Date

2017-09-04

DOI

10.1084/jem.20161122

Peer reviewed

Blimp-1–dependent and –independent natural antibody production by B-1 and B-1–derived plasma cells

Hannah P. Savage,[1,2] Vanessa M. Yenson,[2] Sanjam S. Sawhney,[3] Betty J. Mousseau,[4] Frances E. Lund,[4] and Nicole Baumgarth[1,2,3]

[1]Graduate Group in Immunology, [2]Center for Comparative Medicine, and [3]Department of Pathology, Microbiology, and Immunology, School of Veterinary Medicine, University of California, Davis, Davis, CA
[4]Department of Microbiology, University of Alabama at Birmingham, Birmingham, AL

Natural antibodies contribute to tissue homeostasis and protect against infections. They are secreted constitutively without external antigenic stimulation. The differentiation state and regulatory pathways that enable continuous natural antibody production by B-1 cells, the main cellular source in mice, remain incompletely understood. Here we demonstrate that natural IgM-secreting B-1 cells in the spleen and bone marrow are heterogeneous, consisting of (a) terminally differentiated B-1–derived plasma cells expressing the transcriptional regulator of differentiation, Blimp-1, (b) Blimp-1^{+}, and (c) Blimp-1^{neg} phenotypic B-1 cells. Blimp-1^{neg} IgM-secreting B-1 cells are not simply intermediates of cellular differentiation. Instead, they secrete similar amounts of IgM in wild-type and Blimp-1–deficient (PRDM-1$^{\Delta Ex1A}$) mice. Blimp-1^{neg} B-1 cells are also a major source of IgG3. Consequently, deletion of Blimp-1 changes neither serum IgG3 levels nor the amount of IgG3 secreted per cell. Thus, the pool of natural antibody-secreting B-1 cells is heterogeneous and contains a distinct subset of cells that do not use Blimp-1 for initiation or maximal antibody secretion.

The Journal of Experimental Medicine

INTRODUCTION

Natural antibodies are distinct from the antibodies generated in response to infections. They are of the IgM and, to a lesser extent, class-switched isotypes, such as IgG3. IgM is unique among the antibody classes. It is highly evolutionarily conserved and can be found in all living jawed vertebrates (Flajnik, 2002). IgM secretion begins even before birth (van Furth et al., 1965), independent of all foreign antigen exposure, including exposure to microbiota (Bos et al., 1988; Haury et al., 1997). In contrast, class-switch recombination to IgG1, IgG2, and IgA is strongly enhanced after foreign antigen exposure, explainingreductions of these antibody isotypes in germ-free animals (Bos et al., 1988, 1989). Natural antibody-secreting B-1 cells appear to be specifically selected for self-reactivity (Hayakawa et al., 1999).

Natural IgM has several important protective functions. It suppresses autoantibody production by regulating B cell development and selection (Nguyen et al., 2015) and through clearance of self-antigens, such as cellular debris and apoptotic cells (Boes et al., 2000; Ehrenstein et al., 2000; Notley et al., 2011; Nguyen et al., 2015). It also protects against bacterial and viral infections (Boes et al., 1998; Ochsenbein et al., 1999; Baumgarth et al., 2000; Alugupalli et al., 2003; Haas et al., 2005; Choi and Baumgarth, 2008). It is still unclear, however, how natural IgM secretion is induced and regulated. Yet to harness the therapeutic potential of natural IgM, the cellular sources must be identified.

Several properties of natural IgM antibody-secreting cells (ASCs), including their phenotypes, the tissues they reside in, and their differentiation states, are subjects of debate. Lalor et al. (1989) demonstrated through the use of Ig allotype disparate chimeras that B-1 cells, not conventional B-2 cells, are the main source of natural IgM secretion. Although many other studies have supported these findings (Baumgarth et al., 1999; Ohdan et al., 2000; Haas et al., 2005; Choi and Baumgarth, 2008; Gil-Cruz et al., 2009; Holodick et al., 2009; Choi et al., 2012), a recent study by Reynolds et al. (2015) suggested that fetal- but non-B-1 cell–derived plasma cells (PCs) in the BM are responsible for all natural IgM secretion. Others have found that marginal zone B cells are a source of some natural IgM (Ichikawa et al., 2015).

Among B-1 cells, some researchers have reported that CD5^{+} B-1a cells are the major source of natural IgM (Haas et al., 2005; Holodick et al., 2009), whereas others have suggested that CD5^{neg} B-1b cells are more important (Ohdan et al., 2000; Gil-Cruz et al., 2009). The contributions of peritoneal cavity versus spleen and BM B-1 cells to steady-state natural IgM production have also been debated (Van Oudenaren et al., 1984; Ohdan et al., 2000; Watanabe et al., 2000; Tumang et al., 2005; Holodick et al., 2010; Choi et al., 2012; Reynolds et al., 2015).

Correspondence to Nicole Baumgarth: nbaumgarth@ucdavis.edu

V.M. Yenson's present address is Quintiles, Chatswood, Australia.

Abbreviations used: ASC, antibody-secreting cell; Blimp, B lymphocyte–induced maturation protein; PC, plasma cell.

The Rockefeller University Press
J. Exp. Med. 2017 Vol. 214 No. 9 2777–2794
https://doi.org/10.1084/jem.20161122

Natural IgM-secreting cells produce constant serum levels of IgM throughout life, but the mechanisms of their maintenance are unknown. Terminal differentiation to the PC state after induction of B lymphocyte–induced maturation protein 1 (Blimp-1) is required for the generation of long-lived B-2 cell–derived PCs (Shapiro-Shelef et al., 2003; Kallies et al., 2007). The importance of Blimp-1 for B-1 cell natural IgM production is less clear. Although Tumang et al. (2005) found that B-1 cells secrete IgM independently of Blimp-1, Savitsky and Calame (2006) and Fairfax et al. (2007) reported that B-1 cells require Blimp-1 for secretion. Mice with Blimp-1–deficient B cells have reduced serum levels of natural IgM (Savitsky and Calame, 2006). It is unclear why Blimp-1 deficiency causes reductions rather than loss of natural IgM, but this could be due either to decreased IgM secretion among all natural IgM ASCs or decreased secretion by some (but not all) ASCs. The first possibility is consistent with the role of Blimp-1 in B-2 cells (Nutt et al., 2015) but is difficult to reconcile with the need of B-1 cells for maintenance via self-renewal (Lalor et al., 1989). Interestingly, sharks seem to have two populations of natural IgM-secreting cells that differ in Blimp-1 expression (Castro et al., 2013), providing an evolutionary precedent for Blimp-1–independent generation of IgM secretion.

Less is known about natural IgG3. A recent study reported on the presence of anticommensal IgG3 (Koch et al., 2016), but natural IgG3–secreting cells in germ-free mice (Van Oudenaren et al., 1984; Bos et al., 1988) have been reported as well. B-1 cell–deficient Btk knockout mice lack serum IgG3, suggesting B-1 cells as a possible source (Khan et al., 1995). However, secretion of IgG3 has been studied primarily as a T-independent antibody formed early during an immune response (Perlmutter et al., 1978; Mongini et al., 1981; Gavin et al., 1998; Honda et al., 2009; Colombo et al., 2010). The source of natural IgG3 ASCs and the regulation of their differentiation have not yet been studied.

Our study revealed the coexistence of two main B-1 lineage–derived natural ASC types in the BM and spleens of mice: $CD19^{neg}$ $CD138^{+}$ $Blimp\text{-}1^{hi}$ PCs (B-1PCs) and classical, mostly $CD138^{neg}$ B-1 cells. Although the former are dependent on Blimp-1 for maximal natural Ig production, only some IgM-secreting B-1 cells express and require Blimp-1; most IgG3-producing cells neither express Blimp-1 nor require it for steady-state antibody production. Thus, natural antibody production is provided by multiple B-1 lineage–derived subsets of ASCs, some maximally producing antibodies without Blimp-1–mediated terminal differentiation.

RESULTS

Natural IgM is secreted by B-1 cells and PCs in the spleen and BM

We first investigated natural antibodies in adult, germ-free mice. Consistent with previous studies showing that natural IgM is produced independently of exposure to microbiota (Bos et al., 1988; Haury et al., 1997), serum IgM concentrations, as measured by ELISA, were comparable between SPF and germ-free mice, as were the levels of IgG3, whereas IgA concentrations had decreased as expected (Fig. 1 A). Consistent with the serum antibody levels, frequencies of IgM-secreting cells in the spleen and BM were comparable between SPF and germ-free mice (Fig. 1 B), whereas they were rare in the peritoneal cavity of both types of mice, consistent with previous findings (Ohdan et al., 2000; Watanabe et al., 2000; Choi et al., 2012). We define the IgM and IgG3 present in germ-free mice as "natural antibodies" and conclude that spontaneous IgM and IgG3 secretion of SPF-housed mice largely represents natural IgM and IgG3 generation.

To conduct an unbiased analysis of the major tissue sources of natural IgM ASCs, we compared spontaneous IgM secretion in multiple organs using ELISPOT. Consistent with the results of previous studies (Van Oudenaren et al., 1984; Bos et al., 1988; Choi et al., 2012) but in contrast to the results of the study conducted by Reynolds et al. (2015), the data revealed that both the spleen and BM contain the highest fractions of IgM ASCs (Fig. 1 C, left), whereas other tissues contribute less than 5%. Thus, the spleen and BM are the two main sites of natural IgM secretion. The ELISPOT assay did not record simply "shedding" of surface-expressed IgM BCR, as IgM ELISPOTs were absent after culture of spleen and BM from $\mu s^{-/-}$ mice, which express the IgM BCR but lack secreted IgM (Fig. 1 C, right).

To identify and characterize natural IgM-secreting cells, we FACS-sorted live cells from both the spleen and BM that either did or did not express CD43 and lacked expression of lineage markers for T cells (Thy1), macrophages (F4/80), granulocytes (Gr-1), and natural killer cells (NK1.1; referred to as "dump" markers). In the B cell lineage, CD43 is expressed on PCs and on B-1 cells, two sources previously implicated as main producers of natural IgM (Lalor et al., 1989; Choi et al., 2012; Holodick et al., 2014; Reynolds et al., 2015). Confirming the results of those previous studies, $CD43^{neg}$ cells did not form IgM ASCs in the BM, and only a very small percentage (0.2%) formed ASCs in the spleen (unpublished data). We therefore focused exclusively on the $CD43^{+}$ cell compartment. Further separation of $CD43^{+}$ cells into four subsets based on expression of CD19 and IgM (Fig. 1 D) demonstrated that IgM secretion was restricted to surface IgM^{+} cells (Fig. 1 E), as previously noted (Reynolds et al., 2015). Among those, both $CD19^{+}$ and $CD19^{neg}$ cells contained IgM-secreting cells. The $CD19^{neg}$ fraction made up $0.08 \pm 0.06\%$ of the $CD43^{+}IgD^{neg}$ cells in the BM and made up $0.5 \pm 0.01\%$ in the spleen. Almost all formed IgM ASCs by ELISPOT (Fig. 1 E). The $CD19^{+}$ fraction made up $5 \pm 1\%$ of the $CD43^{+}IgD^{neg}$ cells in the BM and made up $36 \pm 5\%$ in the spleen. Of the $CD19^{+}$ fraction, $0.5 \pm 0.2\%$ in the BM and $4 \pm 0.3\%$ in the spleen formed IgM ASCs (Fig. 1 E).

The $CD19^{neg}IgM^{+}$ cells expressed the PC marker CD138 (Fig. 1 F). This population of $CD19^{neg}IgM^{+}CD43^{+}IgD^{neg}CD138^{+}$ PCs in the BM is similar to that recently identified by Reynolds et al. (2015) as natural IgM PCs.

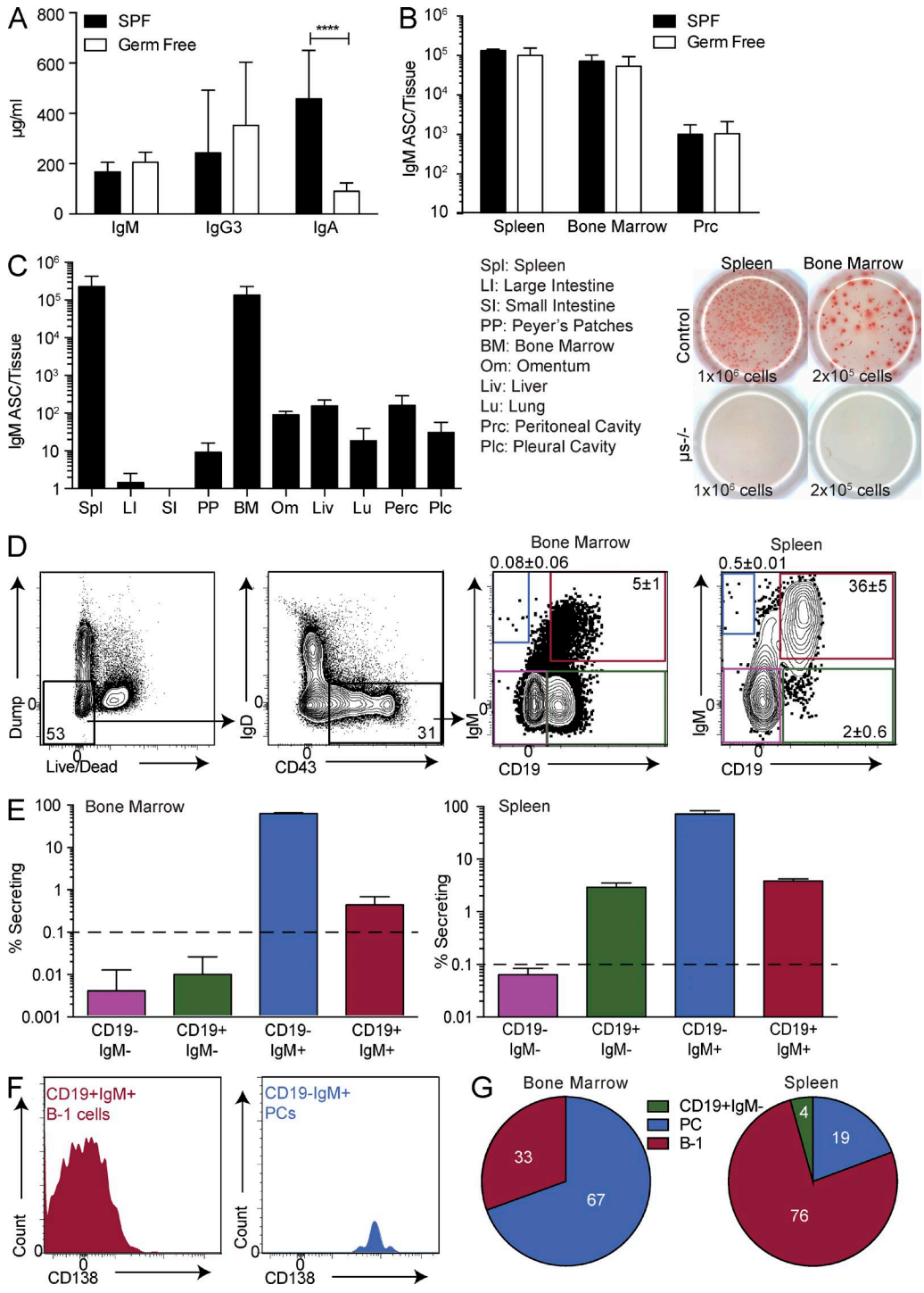

Figure 1. **Phenotypic B-1 cells and PCs secrete natural IgM predominantly in the spleen and BM.** (A) Concentration ± SD (µg/ml) of IgM, IgG3, and IgA in serum of germ-free and SPF-maintained Swiss Webster mice (n = 8–15) measured by ELISA. (B) Number ± SD of IgM ASCs as determined by ELISPOT (n = 7 for germ-free mice and n = 4 for SPF mice). Results are combined (A) or representative (B) of two independent experiments. (C, left) Number ± SD of IgM ASCs in multiple tissues of wild-type neonatal chimeras as measured by ELISPOT (n = 3–6). IgM^a and IgM^b spots were added for each mouse. (C, right) Representative ELISPOT demonstrating IgM secretion by spleen and BM cells of C57BL/6 control mice and mice lacking secretory IgM (µs−/− mice; n = 3). Numbers indicate total input cells. Representative of two independent experiments. (D) Gating strategy for $CD19^+$ $IgM^{+/neg}$ cells after selecting "nondump," $CD43^+$, $IgD^{lo/neg}$ cells. Values shown in all FACS plots represent percentage within parent population. (E) Frequency ± SD of IgM ASCs among live, nondump, $CD43^+$, $IgD^{lo/neg}$ cells in BM (n = 2 for $CD19^{neg}IgM^+$; n = 5 for the others) and spleen (n = 6–7 for IgM^+; n = 2–3 for IgM^{neg}). The dashed lines indicate limit of detection. Results are representative of two independent experiments. (F) Representative FACS histograms of CD138 expression among BM $CD19^+IgM^+$ (B-1

In contrast, among the $CD19^+IgM^+$ cells in the BM and spleen, most were $CD138^{low}$ or $CD138^{neg}$. Their phenotype ($CD19^+CD43^+IgM^+IgD^{neg/lo}$) was that of B-1 cells, which have previously been shown to generate natural IgM (Choi et al., 2012). Thus, we found two major natural IgM secretors: $CD19^{neg}IgM^+CD43^+IgD^{neg}CD138^+$ and $CD19^+CD43^+$, mostly $CD138^{neg}$ B-1 cells. Because B-1 cells are more plentiful than PCs in both the spleen and BM, when both the frequency in each tissue and the frequency of ASC formation among those are considered, B-1 cells formed a mean of 33% of the IgM ASCs in the BM and 76% in the spleen (Fig. 1 G). Thus, we conclude that natural IgM is generated from two cell sources: PCs and classical B-1 lymphocytes.

Natural IgM-secreting B-1 cells and PCs originate from the same population

Previous studies on chimeric mice depleted of B cells and reconstituted at birth with B-1 cells of a different Ig allotype (Lalor et al., 1989) showed that IgM ASCs were mostly from the B-1 cell donor and provided normal levels of serum IgM, suggesting that all natural IgM ASCs are derived from the B-1 lineage. To determine whether natural IgM PCs are B-1 lineage cells, we created neonatal chimeric mice by reconstituting anti-IgM^a–treated CD45.2 Igh^a neonatal recipients with both Ig and CD45 allotype disparate, magnetic bead–purified B-1 cells (Fig. 2 A). After 6 wk of antibody treatment and another 6 wk to allow B-2 cell regeneration, we found that both B-1 cells and $CD19^{neg}IgM^+CD138^+$ PCs were generated from IgM^b- and CD45.1-positive peritoneal cavity B-1 donor cells in BM (Fig. 2 B) and the spleen (Fig. 2 C). Serum analysis showed that the donor-derived B-1PCs and B-1 cells secreted comparable amounts of IgM to those of nonmanipulated control mice (Fig. 2 D). Thus, PCs (B-1PCs) and B-1 cells are repopulated from adult-derived peritoneal cavity B-1 donor cells in neonatal chimeras. The data provide further evidence that most, if not all, natural IgM-secreting cells belong to the B-1 lineage and demonstrate that some B-1 cells undergo terminal PC differentiation.

The majority of B-1 cells lack Blimp-1 expression

Terminal differentiation, regulated by increased expression of the transcriptional regulator Blimp-1 (Shapiro-Shelef et al., 2003), drives increased Ig secretion, suggesting that natural IgM ASCs may express this transcription factor. However, B-1 cells are known to develop primarily from fetal and neonatal cells and to be maintained by self-renewal. Because terminal differentiation would render cells unable to proliferate, we studied Blimp-1 expression among natural IgM-secreting cells using Blimp-1 YFP reporter mice (Rutishauser et al., 2009; Fooksman et al., 2010). In BM and the spleen, the IgM^+ B-1PCs were uniformly Blimp-1 YFP^{hi} (Fig. 3, A and B). In contrast, B-1 cells were almost all Blimp-1 YFP^{neg} in the BM (Fig. 3 A), whereas the spleen contained a small percentage of Blimp-1 YFP-expressing B-1 cells (Fig. 3 B).

We next looked at Blimp-1 expression and IgM secretion among B-1a and B-1b cells in BM, the spleen, and a site that contained only a few spontaneous IgM-secreting cells: the peritoneal cavity (Fig. 3, C and D). Again, we found very few Blimp-1^+ B-1 cells in the BM (Fig. 3 D). The spleen contained a small but distinct population of mostly $CD5^{neg}$ B-1b cells that expressed high levels of Blimp-1 (Fig. 3 D). In contrast to the results of a previous study (Tumang et al., 2005), the peritoneal cavity contained a distinct population of mostly $CD5^+$ B-1a cells that expressed intermediate levels of Blimp-1 (Fig. 3 D). Their Blimp-1 expression was lower than that of the splenic B-1b Blimp-1^+ cells (Fig. 3 D). To determine whether these cells might contain a small number of peritoneal cavity IgM ASCs (Fig. 1 C), peritoneal cavity Blimp-1^{int} B-1a cells were sorted for ELISPOT assays. There was no enrichment for IgM secretion (not depicted). Thus, intermediate expression of Blimp-1 is not a marker of IgM ASCs. Furthermore, the frequencies of Blimp-1^{hi}–expressing B-1 cells in BM and the spleen (Fig. 3 E) did not appear to correlate with the frequencies of B-1 cell IgM ASCs identified in each tissue by ELISPOT (Fig. 1 E), suggesting that both Blimp-1^{hi} and Blimp-1^{neg} B-1 cells contribute to natural IgM secretion.

Blimp-1 expression enhances but is not required for natural IgM secretion

To examine the impact of Blimp-1 expression on IgM secretion by B-1 cells, we studied B cell–specific *prdm1*$^{-/-}$ mice. Previous studies had used $CD19^{cre/+}$ *prdm-1*$^{flx/flx}$ mice. However, B-1a cell development is negatively affected when CD19 levels are reduced (Engel et al., 1995; Rickert et al., 1995; Haas et al., 2005) and $CD19^{cre/+}$ mice have reduced CD19 expression due to the replacement of one allele—CD19—by the *Cre* gene. Consistent with these findings, control mice expressing $CD19^{cre/+}$ alone showed a defective B-1 compartment when compared with wild-type C57BL/6 mice, but one that was similar to that of $CD19^{cre/+}$ PRDM-$1^{flx/flx}$ mice (Fig. 4, A and B). In addition, $CD19^{cre/+}$–only controls had approximately twofold higher frequencies of B-1PCs compared with C57BL/6 mice (Fig. 4 C). The defect in B cell development in $CD19^{cre/+}$ (with or without PRDM-$1^{flx/flx}$) mice affected B-1 but not B-2 cells (Fig. 4 D). Thus, both the $CD19^{cre/+}$ and $CD19^{cre/+}$ PRDM-$1^{flx/flx}$ mice harbored abnormal B-1 cell pools and are ill-suited for B-1 cell studies.

We therefore chose to study PRDM-$1^{\Delta Ex1A}$ mice. These mice lack exon 1 of *prdm1*, which contains the B

cells) and $CD19^{neg}$ IgM^+ (PCs). (G) Contribution of B-1 cells and PCs to total IgM ASCs in indicated tissues was determined by multiplying the percentage of IgM ASCs in each population by the frequency of that population in the tissue ($n = 9$). Results are combined from three to four independent experiments. Statistics in A and B were done using an unpaired Student's *t* test (****, $P < 0.00005$).

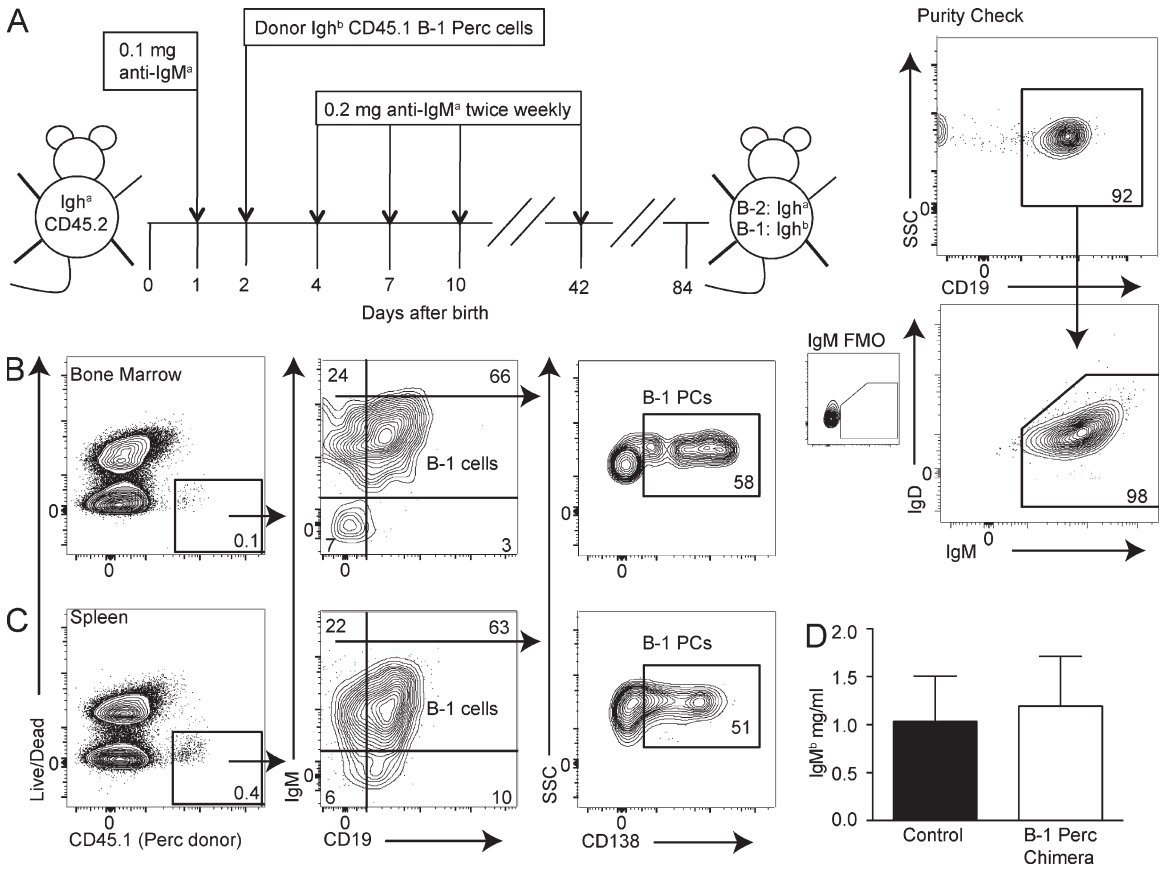

Figure 2. **Natural IgM-secreting PCs are of B-1 cell origin.** (A, left) Neonatal chimeras were created to differentiate B-1 and B-2 cells and their secreted product by their Ig allotype. Neonatal Igh^a/CD45.2 C57BL/6 mice were treated from birth for 6 wk with anti-IgM^a (DS.1) and received magnetic bead (autoMACS)–enriched donor Igh^b/CD45.1 peritoneal cavity cells (PerC, right) within a few days of birth. Values shown in all FACS plots represent percentage within parent population. FMO, fluorescence minus one control stains for IgM. After the end of treatment, mice are rested for at least another 6 wk to allow for B-2 cell reconstitution. Resulting chimeras have IgM^b/CD45.1 donor B-1 cells and IgM^a/CD45.2 host B-2 cells. (B and C) Shown are 5% contour FACS plots of Ig allotype chimeric mice with CD45.2 IgM^a conventional B cells and (CD45.1, IgM^b) peritoneal cavity donor B-1 cells. (B) BM and (C) spleen PC and B-1 cells among CD45.1+ cells. Plots are representative of three mice. (D) B-1–derived serum IgM^b concentrations ± SD (mg/ml) of chimeras and control C57BL/6 (IgM^b) nontreated mice as measured by ELISA ($n = 3$). No significant difference between groups, as assessed by an unpaired Student's t test. Results in B and D are representative of three independent experiments, two of which used FACS-sorted B-1 cells in place of autoMACS-purified B-1 cells.

cell–specific *prdm-1* promoter (Morgan et al., 2009). FACS analysis demonstrated minimal effects on B cell populations of this knockout in a steady state. B-1a and total B-1 cells in the spleens and BM of PRDM-1$^{\Delta Ex1A}$ mice were comparable to those of wild-type mice (Fig. 4, A–C; and Fig. 5 C) but distinct from those with CD19 haploinsufficiency (Fig. 4, A–C). B-1PC populations were reduced in some, but not all, analyses (Figs. 4 C and 5 C). BM B cell development also appeared to be unaffected (Fig. 5 A), resulting in overall normal frequencies of splenic transitional, follicular, and marginal-zone B cell frequencies (Fig. 5 B). Both the CD19$^{cre/+}$ PRDM-1$^{flx/flx}$ and the PRDM-1$^{\Delta Ex1A}$ mice harbored B-1PCs, which in wild-type mice express high levels of Blimp-1. However, B-1PCs in the PRDM-1$^{\Delta Ex1A}$ mice had increased turnover rates compared with the B-1PCs of controls (Fig. 5, D and E), indicating their shortened life spans, as reported previously for B-2PCs (Kallies et al., 2007).

As expected, and in contrast to peritoneal cavity B-1 cells from control C57BL/6 mice and from Blimp-1 YFP reporter mice, B-1 cells from PRDM-1$^{\Delta Ex1A}$ mice did not up-regulate *prdm1* after stimulation with LPS in vitro (Fig. 5 F). This was assessed by qRT-PCR for exon 6 of Blimp-1, which is present in all Blimp-1 transcripts. Previous studies had shown the lack of Blimp-1 protein expression in B cells by Western blot (Morgan et al., 2009). Thus, exon 1 deletion did not lead to transcription of *prdm1* from other start sites in PRDM-1$^{\Delta Ex1A}$ B cells. The cultured PRDM-1$^{\Delta Ex1A}$ cells secreted less IgM, both with and without stimulation, compared with cells from Blimp-1 YFP and C57BL/6 control mice (Fig. 5 G), the latter showing comparable Blimp-1 gene expression and IgM production (Fig. 5, F and G). Importantly, however, PRDM-1$^{\Delta Ex1A}$ B-1 cells did strongly increase IgM production after LPS stimulation with fold inductions similar to those of C57BL/6 controls (133× in controls vs. 164× in

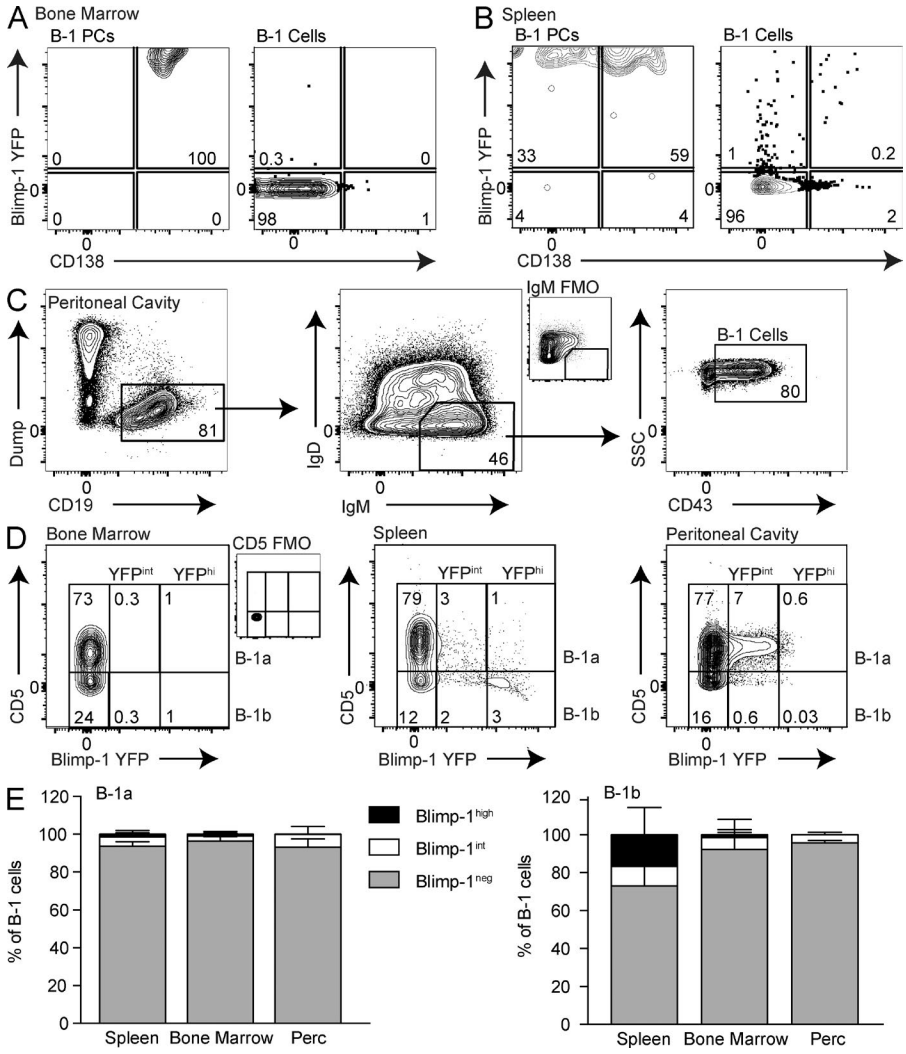

Figure 3. **The majority of B-1 cells lack Blimp-1 expression.** Representative FACS plots showing YFP (Blimp-1) and CD138 staining among CD19^{neg} IgM^{+}CD43^{+} B-1PC and CD19^{+}IgM^{+} IgD$^{lo/neg}$ CD43^{+} B-1 cells in (A) BM and (B) the spleen. Values shown in all FACS plots represent percentage within parent population. (C) Representative FACS gating for peritoneal cavity B-1 cells. (D) Blimp-1 YFP expression among B-1 cells in BM, spleen, and peritoneal cavity was defined as either negative, intermediate, or high. FMO, fluorescence minus one control stains for IgM (C) and CD5 (D), respectively. (E) Frequency ± SD of Blimp-1 YFP high, intermediate, and negative cells among B-1a (left) and B-1b (right) cells in the spleens, BM, and peritoneal cavities of C57BL/6 mice (n = 4–10). Results are pooled from at least three independent experiments.

PRDM-1$^{\Delta Ex1A}$ mice; Fig. 5 G). Thus, peritoneal cavity B-1 cells from PRDM-1$^{\Delta Ex1A}$ mice, although they secreted less IgM after LPS stimulation than their wild-type counterparts, nonetheless significantly increased IgM secretion in response to LPS stimulation without up-regulating Blimp-1.

Consistent with reductions in total IgM secretion in vitro and consistent with the results of a previous study (Shapiro-Shelef et al., 2003), PRDM-1$^{\Delta Ex1A}$ mice had two- to threefold reduced serum IgM levels compared with the controls (Fig. 5 H). Thus, Blimp-1 expression is required for some, but not all, natural IgM secretion. To test whether B-1 cell-intrinsic Blimp-1 expression is required for natural IgM secretion in vivo, we generated neonatal Ig allotype chimeras by reconstituting B cell–depleted Igh^{a} wild-type mice with allotype-mismatched peritoneal cavity B cells from either the controls or PRDM-1$^{\Delta Ex1A}$ (both Igh^{b}) mice. Mice reconstituted with the PRDM-1$^{\Delta Ex1A}$ B-1 cells had significant reductions of serum IgM^{b} levels compared with those reconstituted with control B-1 cells. As expected, the host cell compartment contributed similar small amounts of IgM in both groups (Fig. 5 I). Thus, the decreased natural serum IgM levels in the PRDM-1$^{\Delta Ex1A}$ mice are due to a lack of Blimp-1 expression in the B-1 compartment. Significant levels of serum IgM remained in both PRDM-1$^{\Delta Ex1A}$ mice (Fig. 5 H) and chimeric mice, with Blimp-1 deficiency only in the B-1 compartment (Fig. 5 I).

To determine whether the IgM secreted in PRDM-1$^{\Delta Ex1A}$ mice is functional or qualitatively different from the IgM secreted in control mice, we infected mice with the influenza virus, against which natural IgM is protective (Baumgarth et al., 2000). Viral load was increased ~100-fold in the PRDM-1$^{\Delta Ex1A}$ mice compared with the controls at 24 h after infection (Fig. 5 J). However, when B cell–deficient μMT mice were injected with equal amounts of IgM from either the control or PRDM-1$^{\Delta Ex1A}$ mice, viral lung loads were reduced to similar levels compared with nonreconstituted μMT mice (Fig. 5 K). Thus, natural IgM secreted in the absence of Blimp-1 expression is functional and can neutralize the influenza virus comparably to that of Blimp-1–dependent IgM.

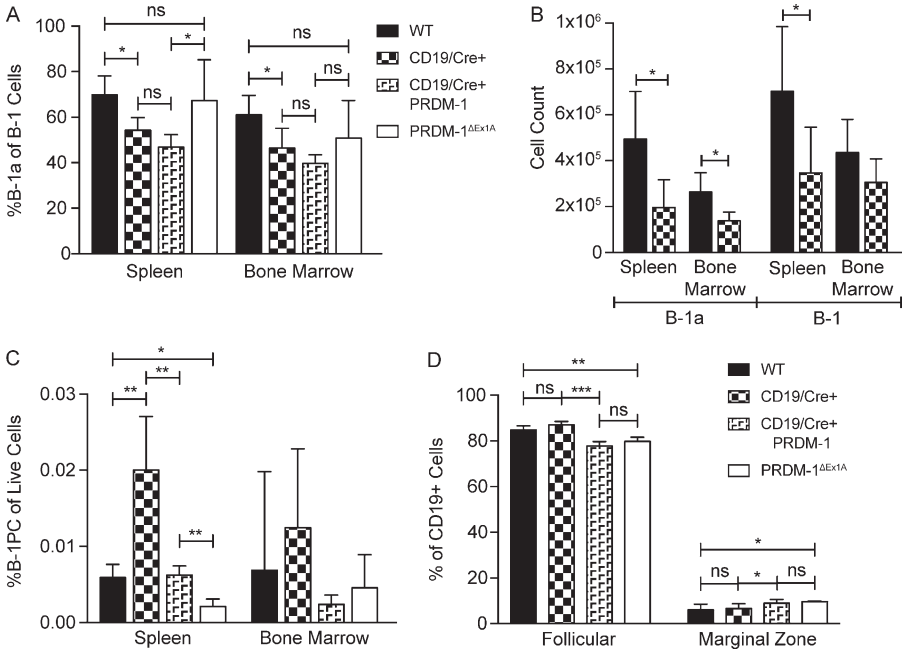

Figure 4. **CD19$^{cre/+}$ PRDM1$^{flox/flox}$ mice are a poor model for B-1–specific knockouts.** (A–D) FACS analysis of the spleens and BM of wild-type (C57BL/6), CD19$^{cre/+}$, CD19$^{cre/+}$ PRDM1$^{flox/flox}$, and PRDM-1$^{\Delta Ex1A}$ mice (n = 4–5). Results are representative of two independent experiments. (A) Frequencies ± SD of B-1a among B-1 cells and (B) the number ± SD of B-1a cells and total B-1 cells. (C) Frequencies ± SD of B-1PCs among live cells and of (D) follicular and marginal zone B-1 cells among B cells in the spleen. All statistics were done using an unpaired Student's t test (*, $P < 0.05$; **, $P < 0.005$; ***, $P < 0.0005$).

Identification of splenic natural IgM ASC subsets with differing requirements for Blimp-1

Decreased serum IgM concentrations in the PRDM-1$^{\Delta Ex1A}$ mice could be explained by reduced natural IgM production per ASCs, similar to the dose effects of Blimp-1 for B-2–derived ASCs (Shapiro-Shelef et al., 2003). Alternatively, Blimp-1–dependent ASCs might be lost in these mice, whereas Blimp-1–independent IgM production remains intact.

To distinguish between these possibilities, we first studied the role of Blimp-1 in the spleen, which contains both Blimp-1^{hi} B-1PCs and a distinct population of Blimp-1^{hi} B-1b cells (Figs. 3 and 6 A). Additionally, we separated these populations into B-1a and B-1b cells because they demonstrated distinct Blimp-1 expression patterns (Fig. 3, D and E). A much higher frequency of Blimp-1^{hi} B-1 cells, both B-1a and B-1b, formed IgM ASCs compared with the Blimp-1^{neg} cells. However, a subset of Blimp-1^{neg} B-1 cells also formed IgM ASCs (Fig. 6 B). Among the Blimp-1^{hi} B-1 cells, B-1b cells formed more ASCs than B-1a cells (Fig. 6 B) and were able to secrete more IgM per cell, as indicated by the larger maximum spot size on ELISPOT (Fig. 6 C). Interestingly, Blimp-1 expression levels among Blimp-1^{+} B-1b cells were higher than those of B-1a cells (Fig. 6 D), consistent with a dose-dependent effect of Blimp-1 expression on the secretory ability of this B-1 subset, similar to that seen in B-2 cells (Shapiro-Shelef et al., 2003). Thus, many, but not all, B-1 cells in the spleen rely on Blimp-1 expression for IgM secretion. A distinct population of splenic B-1 cells exists that seems to neither express Blimp-1 nor rely on this transcriptional regulator for IgM secretion.

Consistent with those data, splenic IgM ASCs were decreased in the PRDM-1$^{\Delta Ex1A}$ mice (Fig. 6 E). Chimeric mice established with either control or PRDM-1$^{\Delta Ex1A}$ Igh^{b} B-1 peritoneal cavity donor cells confirmed that the decrease in IgM ASCs was due to decreased ASC formation by B-1 lineage–derived cells (Fig. 6 F). Correspondingly, IgM secretion in cultures established with cells from the PRDM-1$^{\Delta Ex1A}$ chimeric mice showed a significant reduction compared with the controls (Fig. 6 G). Although overall ASC formation decreased, some cells were able to secrete normal amounts of IgM, as shown by similar maximum ELISPOT spot sizes between control and PRDM-1$^{\Delta Ex1A}$ mice (Fig. 6 H). Thus, the decreases in serum IgM in PRDM-1$^{\Delta Ex1A}$ mice are due to reduced IgM secretion by some Blimp-1–dependent IgM ASCs, whereas other Blimp-1–independent IgM ASCs secrete normally.

We then examined whether the decrease in ASC formation in the PRDM-1$^{\Delta Ex1A}$ mice was due chiefly to a reduction in the uniformly Blimp-1^{hi}–expressing CD19^{neg}IgM^{+}CD138^{+} B-1PCs (Fig. 3 A). Both B-1PC and B-1 cells were present in PRDM-1$^{\Delta Ex1A}$ mice, yet IgM ASC frequencies were decreased approximately twofold among both populations (Fig. 6 I). B-1PC and B-1 cells were also sorted from $\mu s^{-/-}$ mice and no spots were seen, demonstrating that the observed spots are not due to surface IgM shedding (not depicted). Because B-1a and B-1b cells differed in Blimp-1 expression levels, we performed ELISPOT analysis separately on sorted B-1a and B-1b cells. B-1b IgM ASC formation was greatly decreased in the PRDM-1$^{\Delta Ex1A}$ mice (Fig. 6 J), consistent with the higher frequency of splenic IgM ASCs among Blimp-1^{+} B-1b cells compared with other B-1 cell populations (Fig. 6 B). However, among B-1b cells able to form ASCs, both mean and maximal spot sizes were similar to those formed by control cells (Fig. 6 K). Consistently across all experiments, splenic B-1a ASC forma-

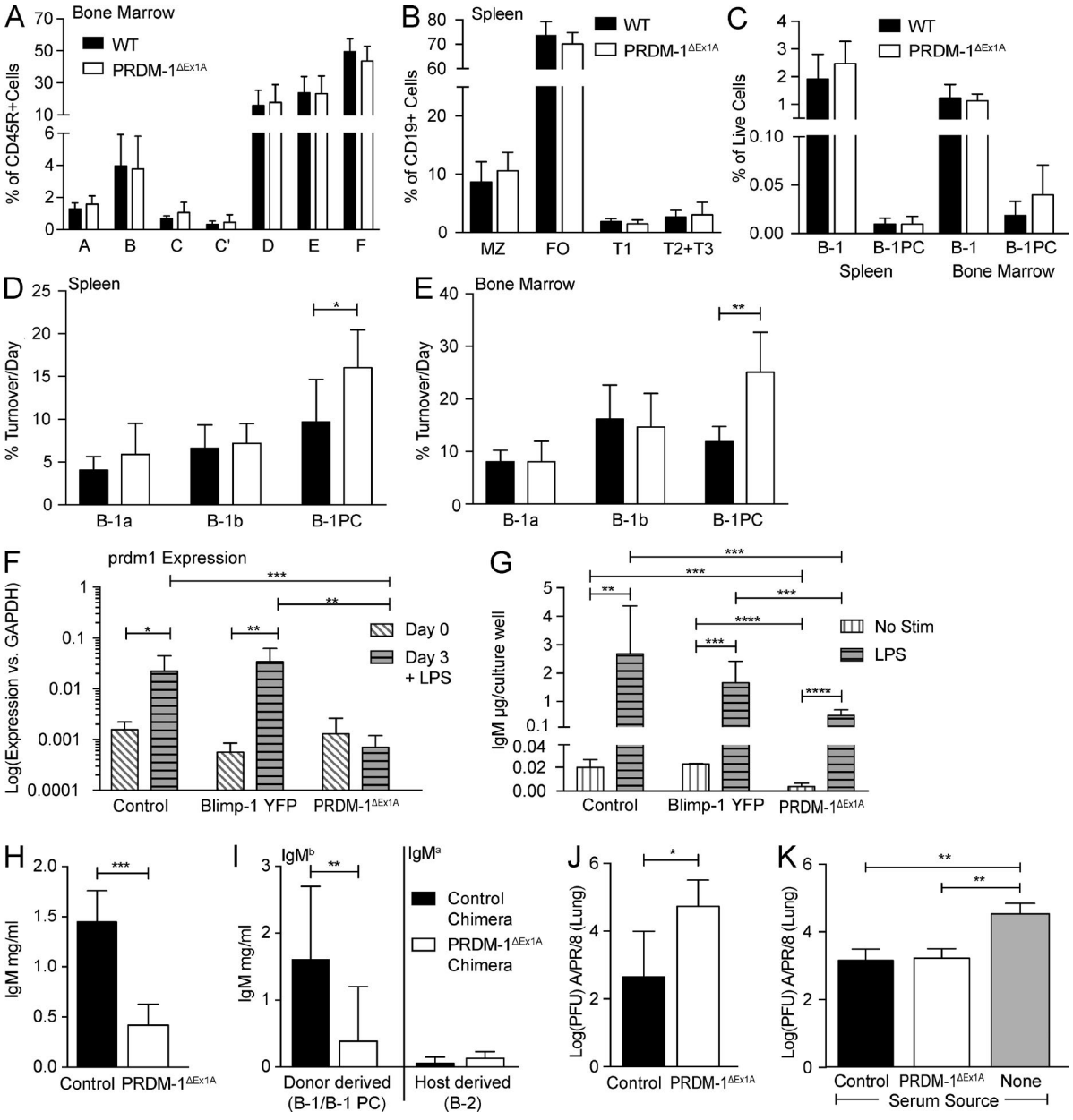

Figure 5. **Blimp-1 expression is not required for natural IgM secretion.** (A-E) FACS analysis of the spleen and BM of C57BL/6 wild-type and PRDM-1$^{\Delta Ex1A}$ mice. Results are pooled from two (A-C, n = 8–9 mice) or three (D and E, n = 6) independent experiments. (A) Mean frequencies ± SD of developing B cells in BM according to the Hardy scheme (Hardy and Hayakawa, 2001): A, prepro; B, pro; C, late pro; C', early pre; D, late pre; E, immature; F, mature B cells. (B) Mean frequencies ± SD of marginal-zone (MZ), follicular (FO), and transitional (T1, T2+T3) spleen B cells. (C) Mean frequencies ± SD of B-1 cells and B-1PCs. Mean percentage of cell turnover per day ± SD of B-1a, B-1b, and B-1PC cells, as determined by BrdU incorporation, in C57BL/6 wild-type and PRDM-1$^{\Delta Ex1A}$ mice in (D) the spleen and (E) BM. (F) Mean relative expression of *prdm1* relative to *gapdh* ± SD as measured by qRT-PCR (n = 3–5 samples). (G) Concentrations of IgM ± SD (µg/ml) in supernatants (n = 6–12), before and after 3-d culture of peritoneal cavity B cells with or without LPS from C57BL/6 control, Blimp-1 YFP, and PRDM-1$^{\Delta Ex1A}$ mice. Results in F and G are pooled from two independent experiments. (H) Mean serum IgM ± SD (mg/ml) in control and PRDM-1$^{\Delta Ex1A}$ mice as determined by ELISA (n = 5–6). Results are representative of more than three independent experiments. (I) Serum IgM^a and IgM^b (mg/ml) ± SD as measured by ELISA (n = 12–14). Sera are from neonatal Ig allotype chimeras with IgM^a wild-type controls, reconstituted with IgM^b-expressing wild-type (control) or PRDM-1$^{\Delta Ex1A}$ peritoneal cavity donor B-1 cells. Results are pooled from three independent experiments. (J) Mean viral loads ± SD (PFUs) in the lungs of control and PRDM-1$^{\Delta Ex1A}$ mice as measured by qRT-PCR 24 h after infection with Influenza A/PR/8 (n = 4). (K) Mean viral loads ± SD (PFUs) in the lungs of µMT mice 24 h after infection. µMT mice were given equal amounts of immune serum IgM from either control or PRDM-1$^{\Delta Ex1A}$ mice or no serum (n = 3–5). Results in J and K are pooled from two independent experiments. All statistics were done using an unpaired Student's t test (*, P < 0.05; **, P < 0.005; ***, P < 0.0005; ****, P < 0.00005).

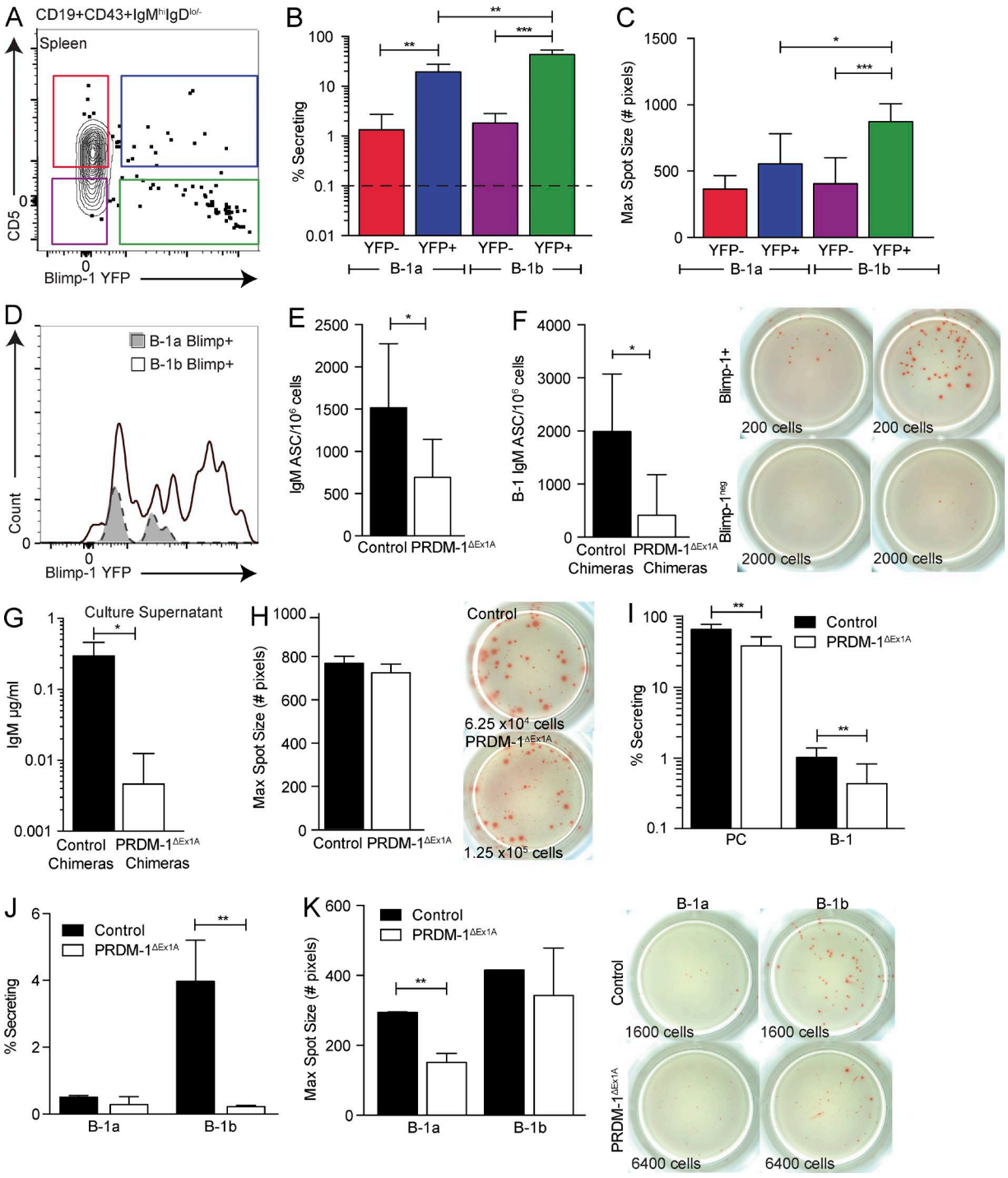

Figure 6. **Identification of subsets of splenic natural IgM ASCs differing in their requirements for Blimp-1.** (A) Sorting gates for Blimp-1 YFP among B-1a and B-1b splenocytes pregated as live, singlet, dump^{neg} CD19^{+}CD43^{+}IgM^{hi}IgD$^{lo/neg}$ cells. (B) Mean frequencies ± SD of IgM ASCs among Blimp-1 YFP^{+} (YFP+) and Blimp-1 YFP^{neg} (YFP-) B-1a and B-1b cells in the spleen (n = 3–8). The dashed line represents the limit of detection. (C, top) Mean maximum IgM spot size ± SD (number of pixels) in each ELISPOT well of sorted Blimp-1 YFP^{+} or YFP^{neg} B-1a and B-1b cells (n = 3–8) and (C, bottom) representative ELISPOT wells. Numbers indicate total input cells. Results in B and C are representative of two independent experiments. (D) Representative overlay histograms of Blimp-1 YFP among YFP^{+} B-1a and B-1b cells. (E) Mean frequencies ± SD of IgM ASC splenocytes from control and PRDM-1$^{\Delta Ex1A}$ mice (n = 11) and (F) control and PRDM-1$^{\Delta Ex1A}$ IgM^{b} peritoneal cavity donor chimeras (n = 4–9) as measured by ELISPOT. Results in E and F are pooled from two independent experiments. (G) B-1–derived IgM ± SD (µg/ml) in supernatants of splenocytes from control and PRDM-1$^{\Delta Ex1A}$ B-1 peritoneal cavity donor chimeras as measured by ELISA (n = 3–5). (H, left) Mean maximum IgM spot size ± SD (number of pixels) in each ELISPOT well for control versus PRDM-1$^{\Delta Ex1A}$ mice

tion was low compared with that of B-1b (Fig. 6 J), and the few existing splenic B-1a ASCs required Blimp-1 for maximal secretion (Fig. 6, B, J, and K). We conclude that many B-1 cells in the spleen require Blimp-1 for maximum IgM secretion, whereas a small subset of B-1b cells secrete IgM independently of Blimp-1, demonstrating heterogeneity in the requirement for Blimp-1 expression among IgM-secreting splenic B-1 cells.

BM B-1PCs, but not B-1 ASCs, require Blimp-1 for maximal IgM secretion

The BM contains Blimp-1 YFP^{+} B-1PCs and largely Blimp-1 YFP^{neg} B-1 cells (Figs. 3 and 7 A). Consistent with those findings, frequencies of FACS-purified IgM ASCs among total BM B-1a and B-1b cells and those depleted of any Blimp-1–expressing cells were comparable (Fig. 7 B). Confirming that YFP expression correlated with *prdm1* gene expression, qRT-PCR analysis conducted on FACS-sorted BM B-1 cells showed the absence of *prdm1* mRNA, whereas PCs expressed *prdm1* and expressed *irf4* at levels higher than those of B-1 cells (Fig. 7 C).

Few genes other than Blimp-1/IRF-4 are known that regulate PC fate. One is *zbtb20* (Chevrier et al., 2014). However, we did not find any difference in *zbtb20* expression comparing nonsecreting follicular B cells with Blimp-1^{+} B-1PCs and BM B-1 cells (Fig. 7 C). Despite this, BM B-1 cells expressed ∼100-fold more mRNA for the J chain than follicular B cells, indicating that they generate pentameric IgM (Fig. 7 C). Further support came from fluorescent imaging studies, which identified BM Blimp-1 YFP^{neg} B-1 cells that contained intracellular IgM vesicles (Fig. 7 D), similar to the Blimp-1 YFP^{+} B-1PCs (Fig. 7 D). Thus, BM B-1 cells secrete IgM in the absence of known transcriptional regulators of PC differentiation.

Unexpectedly, given the strong contribution of B-1PCs to IgM production in BM (Fig. 1 G), the number of IgM ASCs among total BM cells was comparable between the control and PRDM-1$^{\Delta Ex1A}$ mice (Fig. 8 A), as well as in neonatal chimeric mice reconstituted with control or PRDM-1$^{\Delta Ex1A}$ Igh^{b} peritoneal cavity cells (Fig. 8 B). Furthermore, the mean ELISPOT spot sizes formed by BM cells from control and PRDM-1$^{\Delta Ex1A}$ mice were also comparable (Fig. 8 C), as were the overall IgM secretion levels of BM cells in culture (Fig. 8 D). Thus, the lack of Blimp-1 expression in the B-1 cell compartment did not seem to affect the frequencies of BM IgM ASCs, nor the amount of IgM secreted.

This prompted us to separately assess the effects of Blimp-1 deficiency on BM B-1PC and B-1 cells. As predicted, IgM ASC formation was significantly decreased among B-1PCs (Fig. 8 E). However, there was a significant compensatory increase of IgM ASCs among the B-1 cells (Fig. 8 E), explaining the similar IgM ASC numbers in the BM of PRDM$^{\Delta Ex1A}$ and control mice. Sorting of BM B-1a and B-1b cells from the control and PRDM-1$^{\Delta Ex1A}$ mice for ELISPOT analysis confirmed the higher frequencies of IgM ASCs among BM B-1a and B-1b cells in the PRDM-1$^{\Delta Ex1A}$ mice compared with the controls (Fig. 8 F). Their mean ELISPOT spot sizes were similar to those of control mice, indicating similar IgM secretion per cell (Fig. 8 G). Blimp-1 deficiency did not change the absolute number of B-1a and B-1b cells in the BM (Fig. 8 H); instead, the BM B-1 cell compartment appears to respond to reductions in local and/or systemic IgM production with increased antibody secretion without up-regulating Blimp-1.

Natural IgG3 B-1 ASCs do not require Blimp-1 for maximal secretion

Intriguingly, serum IgG3, which is produced in the absence of microbial challenge (Fig. 1 A), was unchanged in PRDM-1$^{\Delta Ex1A}$ mice compared with control mice, whereas other IgG subtypes as well as IgA were decreased (Fig. 9 A). Similarly, IgG3 ASC formations in the spleen and BM were comparable (Fig. 9 B), as were mean ELISPOT spot sizes, indicating similar secretion by individual cells (Fig. 9 C). To determine whether B-1 cells are the source of IgG3, we compared serum IgG3 concentrations in the neonatal chimeras at the end of anti-IgM treatment, when donor-derived B-1 cells are the only B cells present (day 42), and again in the same chimeras after full reconstitution of the conventional B cell pool (day 97). Serum IgG3 levels in each of these mice were similar between day 42 and day 97, strongly indicating that most serum IgG3 is derived from B-1 cells (Fig. 9 D).

Consistent with a lack of Blimp-1 involvement in serum IgG3 production, the vast majority of IgG3^{+} B cells in the spleen lacked Blimp-1 YFP expression (Fig. 9 E, left). IgG3 secretion occurred only among IgG3^{+} cells (Fig. 9 E, right) and among both of those, the few Blimp-1 YFP^{+} and the majority of Blimp-1 YFP^{neg} cells formed IgG3 ASCs (Fig. 9 E, right). The frequencies of YFP^{+} cells exceeded the percentage of secretion seen among the YFP^{neg} cells, excluding contamination with YFP^{+} cells as a trivial explanation for IgG3 secretion in the absence of Blimp-1. The IgG3^{+} YFP^{neg} cells secreted similar amounts per cell compared with the IgG3^{+} YFP^{+} cells, as indicated by their similar spot sizes (Fig. 9 F). Together, our studies identify the significant and unique contributions of Blimp-1–independent B cell ASCs to the production of natural IgG3 and some natural IgM.

(*n* = 3) and (H, right) representative ELISPOT wells. Numbers indicate total input cell numbers. Results are representative of two independent experiments. (I) Mean frequencies ± SD of IgM ASCs among splenic CD19^{neg} IgM^{+} IgD$^{lo/neg}$ CD43^{+} CD138^{+} B-1PC and CD19^{+} IgM^{+} IgD$^{lo/neg}$ CD43^{+} B-1 cells (*n* = 9–10) and of (J) splenic B-1a and B-1b cells (*n* = 2–4) in control and PRDM-1$^{\Delta Ex1A}$ mice. (K, left) Mean maximum IgM spot size ± SD (number of pixels) in each ELISPOT well of sorted Blimp-1 YFP^{+} and YFP^{neg} B-1a and B-1b cells (*n* = 2–4) and (K, right) representative ELISPOT wells. Results in I–K are representative of two independent experiments. Statistics in B and C and E–K were done using an unpaired Student's *t* test (*, P < 0.05; **, P < 0.005; ***, P < 0.0005).

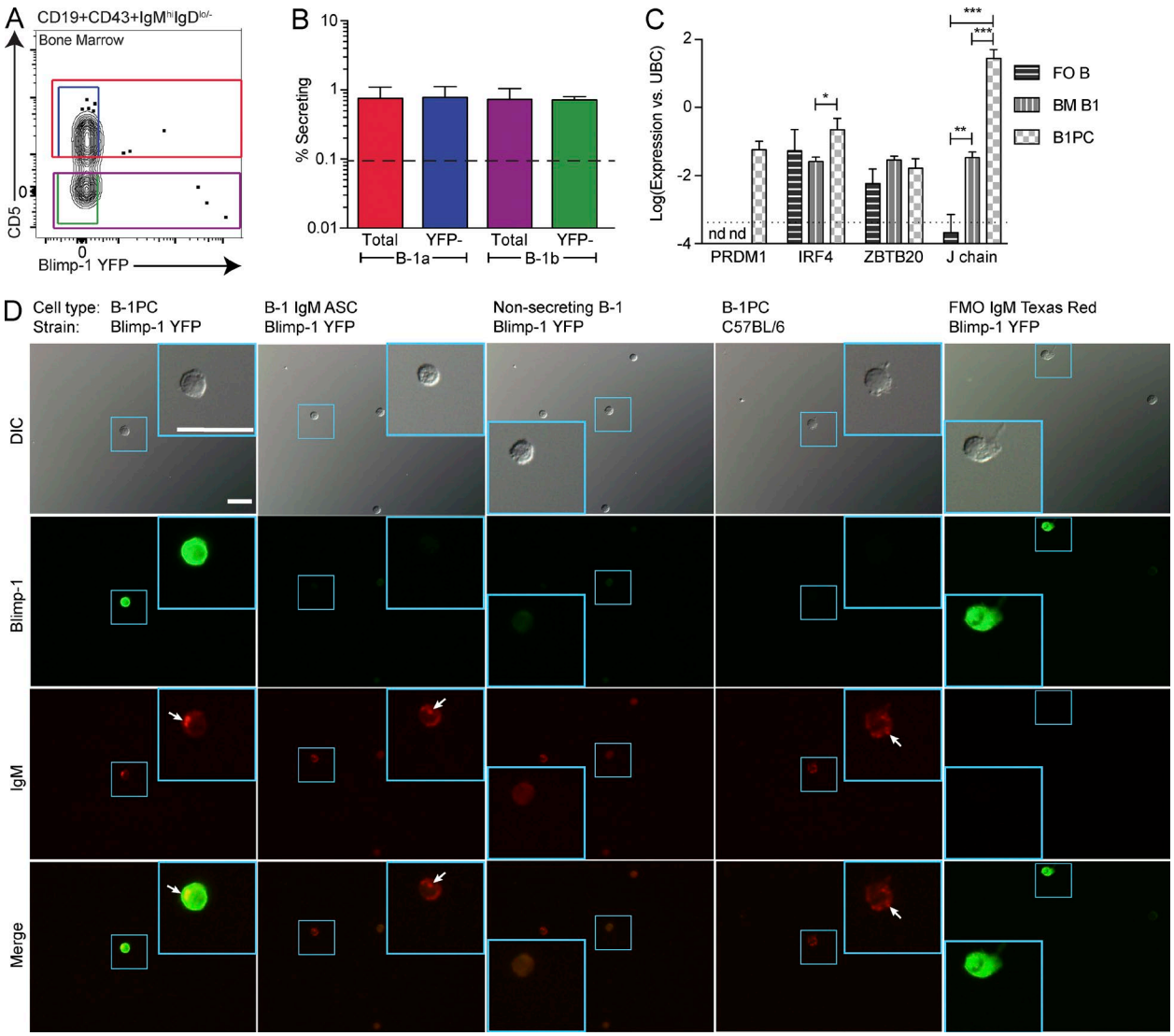

Figure 7. **BM B-1PC, but not B-1 cells, require Blimp-1 for maximal IgM secretion.** (A) Gating for total and Blimp-1 YFP^{neg} (YFP-) B-1a and B-1b BM cells, pregated on live, singlet, dump^{neg}, CD19^{+}CD43^{+}IgM^{hi} IgD$^{lo/neg}$ cells. (B) Mean frequencies ± SD. IgM ASCs among total and Blimp-1 YFP^{neg} B-1a and B-1b cells in the BM (n = 4). The dashed line represents the limit of detection. Results are representative of two independent experiments. (C) *Prdm1*, *irf4*, *zbtb20*, and *igj* (J chain) mRNA expression (Log) ± SD by FACS-sorted follicular B cells (FO B), BM B-1 cells, and B-1PCs, normalized to *ubc* (n = 3). Results are combined from two independent experiments. (D) Fluorescent imaging of (left to right) FACS-sorted B-1PCs (first column) and BM B-1 cells either showing (second column) or not showing (third column) intracellular IgM staining, all taken from Blimp-1 YFP reporter mice and B-1PCs (fourth column) taken from C57BL/6 mice. Top to bottom: differential interference contrast images, Blimp-1 YFP (green), intracellular IgM (red), and merged images. Arrows indicate intracellular IgM vesicles. Smaller blue boxes indicate the magnified area found in the larger blue box in the same image. The scale bars (25 µm) in the top left image apply to all images. FMO, fluorescence minus one control stains for intracellular IgM (fifth column). C57BL/6 B-1PCs serve as FMO for YFP expression and are stained with anti–GFP/YFP-FITC. Images are representative of multiple cells from two independent experiments. Statistics in B and C were done using an unpaired Student's t test (*, $P < 0.05$; **, $P < 0.005$; ***, $P < 0.0005$).

DISCUSSION

Our data identified two distinct sources of natural IgM: classical B-1 cells and B-1–derived PCs. B-1PCs and most splenic B-1 cells resemble B-2 cells in their requirement for Blimp-1 for secretion. However, some classical B-1 cells, particularly those in BM, neither expressed nor required Blimp-1 for secretion. BM, but not splenic B-1 cells, responded to low serum IgM levels by increasing the percentage of cells that secreted IgM, not by increasing IgM production per cell. In PRDM-1$^{\Delta Ex1A}$ mice, this resulted in partial compensation for the loss of Blimp-1–dependent secretion by B-1PCs in the BM, where ASC numbers were comparable between

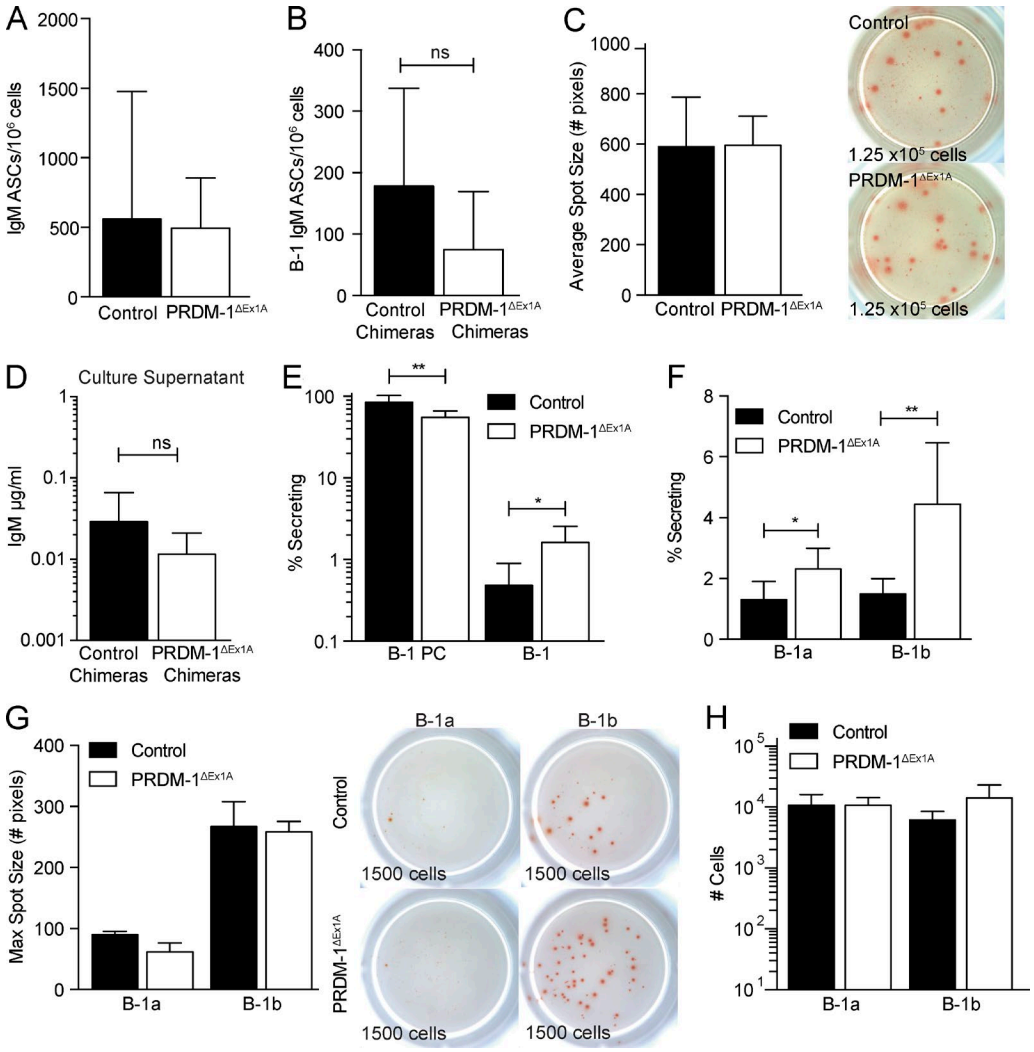

Figure 8. **PRDM-1$^{\Delta Ex1A}$ BM B-1 cells can increase frequencies of IgM ASCs.** (A) Mean frequencies ± SD of IgM ASCs among BM cells from control and PRDM-1$^{\Delta Ex1A}$ mice (n = 11) and (B) control and PRDM-1$^{\Delta Ex1A}$ IgM^{b} peritoneal cavity donor chimeras (n = 4–9). (C, left) Mean spot sizes ± SD (number of pixels) for control and PRDM-1$^{\Delta Ex1A}$ mice (n = 3) and (C, right) representative ELISPOT wells. Numbers indicate total input cell count. Results are representative (A and C) or pooled (B) from two independent experiments. (D) Mean B-1–derived IgM ± SD (µg/ml) in supernatants of cultured BM cells from control and PRDM-1$^{\Delta Ex1A}$ B-1 peritoneal cavity donor chimeras as measured by ELISA (n = 3–5). (E) Mean frequencies ± SD of IgM ASCs among BM CD19^{neg} CD43^{+} IgM^{+} IgD$^{lo/neg}$ CD138^{+} B-1PC and CD19^{+} CD43^{+} IgM^{+} IgD$^{lo/neg}$ B-1 cells and (F) B-1a and B-1b cells in control and PRDM-1$^{\Delta Ex1A}$ mice (n = 5–8). (G, left) Mean maximum IgM spot sizes ± SD (number of pixels) of sorted Blimp-1 YFP^{+} and YFP^{neg} B-1a and B-1b cells (n = 2 for control mice; n = 3 for PRDM-1$^{\Delta Ex1A}$ mice) and (G, right) representative ELISPOT wells. Numbers indicate total input cells. (H) Total numbers ± SD of live BM B-1a and B-1b cells calculated based on total live cell counts and percentages of B-1a and B-1b cells (n = 3). Results in E–H are representative of two independent experiments. Statistics for all panels were done using an unpaired Student's t test (*, $P < 0.05$; **, $P < 0.005$).

PRDM-1$^{\Delta Ex1A}$ and control mice. Surprisingly, IgG3 secretion by B-1 cells was mostly Blimp-1–independent, explaining the normal serum IgG3 levels in PRDM-1$^{\Delta Ex1A}$ mice.

Multiple lines of evidence suggest that Blimp-1^{neg} ASCs are not simply precursors of Blimp-1–expressing cells. First, Blimp-1^{neg} IgM ASCs in BM are able to secrete as much antibody as total BM IgM ASCs, as shown in ELISPOT and in culture experiments, when comparing IgM secretion by B-1 cells from PRDM-1$^{\Delta Ex1A}$ and control mice and comparing sorted Blimp-1 YFP^{pos} and YFP^{neg} B-1 cells. The data indicate that Blimp-1 is not needed for maximal IgM secretion by these cells. Second, most natural IgG3 ASCs lacked Blimp-1 expression and, correspondingly, serum IgG3 levels in PRDM-1$^{\Delta Ex1A}$ mice were comparable to those of the controls. Class switching away from IgM to another isotype requires activation and induction of AID expression (Muramatsu et al., 2000), stimulated by signals mediated through the BCR, TLR, or CD40L (Keim et al., 2013). Thus, IgG3-secreting cells must have received activation signals to class switch to IgG3, yet most remain Blimp-1^{neg}. This suggests that an alter-

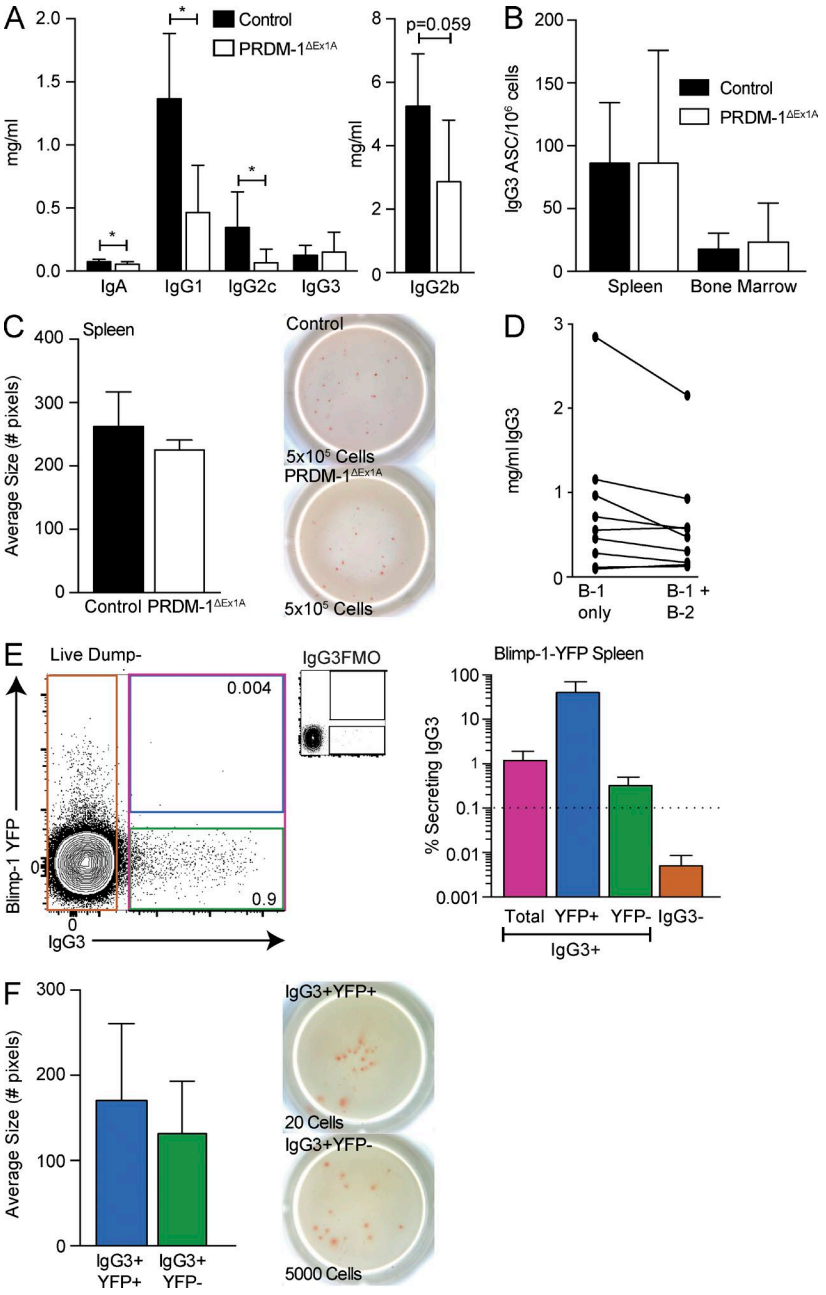

Figure 9. **Natural IgG3 is secreted independently of Blimp-1.** (A) Shown are serum Ig isotype concentrations ± SD (mg/ml) in control and PRDM-1$^{\Delta Ex1A}$ mice (n = 5–9 for IgA, IgG1, IgG2c, and IgG2b; n = 12–15 for IgG3). Results are pooled from two independent experiments. (B) Mean frequencies ± SD of IgG3 ASCs among the spleens and BM from control and PRDM-1$^{\Delta Ex1A}$ mice (n = 3). (C, left) Mean spot sizes ± SD (number of pixels) from IgG3 ASCs in the spleens of control and PRDM-1$^{\Delta Ex1A}$ mice (n = 3) and (C, right) representative ELISPOT wells. Numbers indicate total input cells. Results in B and C are representative of two independent experiments. (D) Serum IgG3 (mg/ml) ± SD in mice with only B-1 cells (neonatal chimeras, day 42, during DS-1 treatment) and in the same mice after reconstitution of B-2 cells (day 94). Each line represents one mouse. Results are combined from two independent experiments. (E, left) Sample gating for total IgG3$^+$ and IgG3^{neg} cells, as well as IgG3$^+$ Blimp-1 YFP$^+$ and YFP^{neg} cells, pregated on live, singlet, and dump^{neg} cells. FMO, fluorescence minus one control stains for IgG3. Values shown in FACS plot represent percentage within parent population. Cells were sorted directly into ELISPOT plates. (E, right) Mean frequencies ± SD of IgG3 ASCs among splenic IgG3$^+$ (total), IgG3$^+$ Blimp-1 YFP$^+$ (YFP+), and IgG3$^+$ YFP^{neg} (YFP-) and IgG3^{neg} cells (n = 4–8). The dashed line represents the limit of detection. (F, left) Mean spot sizes ± SD (number of pixels) from splenic IgG3$^+$ Blimp-1 YFP$^+$ and IgG3$^+$ YFP^{neg} cells (n = 3) and (F, right) representative ELISPOT wells. Results in E and F are representative of three independent experiments. Statistics in A–C and F were done using an unpaired Student's t test (*, P < 0.05).

native activation/differentiation pathway exists that supports antibody secretion and is used in the Blimp-1^{neg} ASCs.

All B-1 cells exhibit signs of activation: They are larger and contain a greater amount of cytoplasm than follicular B-2 cells, consistent with being in an activated state. In contrast to follicular B cells, but similar to plasma blasts, B-1 cells in the spleen and BM express CD43, a marker of B cell differentiation, and they show increased surface expression of the costimulatory molecules CD80/CD86. Because natural IgM secretion is not affected by microbiota or infections, as demonstrated by studies in germ-free mice, the induction of this activation state is likely the outcome of interaction with self-antigens. It is possible that the timing or location of activation by self-antigens, or the specific properties of the self-antigen, determines whether cells will differentiate along the Blimp-1–dependent or Blimp-1–independent pathway. Alternatively, distinct subsets of B-1 cells may exist that differ in their ability to induce Blimp-1.

B-1 cells develop from multiple fetal, neonatal, and adult tissues (Herzenberg et al., 1986; Solvason et al., 1991; Kantor et al., 1992; Godin et al., 1993; Düber et al., 2009; Esplin et al., 2009; Holodick et al., 2009; Ghosn et al., 2012; Kobayashi et al., 2014). They have precursors of both hematopoietic and nonhematopoietic origins (Kantor et al., 1992; Kobayashi et

al., 2014). Whether each of these sources contributes equally to all B-1 cell subsets is unclear. We found that both Blimp-1^{+} and Blimp-1^{neg} natural ASCs can develop from adult peritoneal cavity B-1 cells. When transferred into a neonate lacking B-1 cells, peritoneal B-1 cells are able to reconstitute all subsets of B-1 cells in the spleen and BM, including B-1PCs, Blimp-1–dependent and Blimp-1–independent B-1 IgG3, and IgM ASCs. However, whether an individual B-1 cell precursor can form all of these cells or whether the B-1 precursor population is heterogeneous remains to be studied. Montecino-Rodriguez and Dorshkind (2012) recently proposed that B-1 cells develop in waves arising from the yolk sac, fetal liver, and fetal BM. These waves of B-1 cells could be contributing distinct precursor populations, which develop into cells that phenotypically look very similar but rely on different regulatory pathways for differentiation, to the B-1 cell pool. Castro et al. (2013) reported on a similar dichotomy of Blimp-1 dependence and independence among IgM-secreting cells of the shark. Thus, both the Blimp-1–dependent and Blimp-1–independent pathways of B cell differentiation might be well conserved in evolution.

An important avenue for future exploration raised by these studies is to define the molecular signature of Blimp-1^{neg} ASCs. To address this question, significant technical challenges must be overcome—in particular, the low frequency of these cells among the pool of nonsecreting B-1 cells, as well as the lack of a marker that can cleanly distinguish Blimp-1^{neg}–, IgM–, and IgG3–secreting from nonsecreting cells. Although Blimp-1 is a key molecule of the PC gene network, this does not preclude the presence of other genes regulating antibody secretion by B cells. The fact that IgM-secreting B-1 cells continue to express CD19, a target gene activated by BSAP in B-2 cells but suppressed by Blimp-1 through its repression of BSAP, suggests that antibody-secreting B-1 cells, including those expressing Blimp-1, differ in their transcriptional profile from PCs. Another important function of Blimp-1 is the repression of PAX5, which, among other effects, drives expression of sXBP-1 in support of the unfolded protein response of secreting cells and thus regulates ER stress (Nutt et al., 2015). However, B-1 cells express reduced levels of PAX5 compared with follicular B cells (Tumang et al., 2005; Choi et al., 2012), which may help to facilitate up-regulation of sXBP-1 independent of Blimp-1.

Further studies are required to determine the unique gene expression profile of the natural antibody-secreting Blimp-1^{neg} B cell pool.

In summary, our data demonstrate that a heterogeneous pool of Blimp-1–dependent and Blimp-1–independent natural antibody-secreting B-1 cells contribute to serum IgM and IgG3 production. Further exploration of the differences between these distinct populations of natural ASCs may lead to more targeted therapeutics for diseases and conditions such as autoimmune diseases, atherosclerosis, and chronic inflammation that might be treated through induction of enhanced natural antibody production.

MATERIALS AND METHODS

Mice

8–16-wk-old male and female C57BL/6J mice and breeding pairs of B6.Cg-*Gpi1*^{a}*Thy1*^{a}*Igh*^{a}/J (Igh^{a}), B6.129S2-*Ighm*^{tm1Cgn}/J (μMT), and B6.SJL-*Ptprc*^{a}*Pepc*^{b}/BoyJ (CD45.1) were purchased from The Jackson Laboratory. B6.Cg-Tg(PRDM1-EYFP)1Mnz (Blimp-1 YFP) breeders were provided by M. Nussenzweig (The Rockefeller University, New York, NY). PRDM-$1^{\Delta Ex1A}$ breeders were provided by E. Bikoff (University of Oxford, Oxford, England, UK). B6.129S-sIgM$^{-/-}$ ($\mu s^{-/-}$) breeders were a gift from F. Lund (University of Alabama at Birmingham [UAB], Birmingham, AL). Swiss Webster germ-free mice were provided by A. Bäumler (University of California, Davis [UC Davis], Davis, CA), and age/sex-matched Swiss Webster controls were purchased from Taconic.

For experiments involving $CD19^{cre/+}$ mice, C57BL/6, $CD19^{cre/+}$, and $CD19^{cre/+}$ PRDM-$1^{flx/flx}$ mice were housed at UAB. Mice were of mixed sexes, and all mice were age-matched. Mice were bred and maintained under SPF conditions in microisolator cages and were euthanized by overexposure to carbon dioxide. All procedures and experiments involving animals were approved by the Animal Use and Care Committee of UC Davis and UAB. Unless otherwise indicated, all "control" mice were age- and sex-matched C57BL/6J mice (The Jackson Laboratory) and were housed for at least 1 wk in our mouse facility.

Neonatal chimeric mice were generated as previously described (Baumgarth et al., 1999). In brief, neonatal B6.Cg-Gpi1^{a}Thy1^{a}Igh^{a} mice were injected i.p. with 0.1 mg of DS.1 antibody (anti-IgM^{a}) 1–2 d after birth to deplete host B cells and twice weekly after that for 6 wk. On day 2 or 3 after birth, they received i.p. total peritoneal and pleural cavity lavage cells or highly purified B-1 cells from congenic donor Igh^{b} mice. After the last antibody injection, chimeras were rested for at least 6 wk to allow for host B cell reconstitution. In these mice, most B-1 cells are donor derived (Igh^{b}), whereas all conventional B cells are host derived (Igh^{a}). For PRDM-$1^{\Delta Ex1A}$ chimeras, C57BL/6 mice were used as the donors to make control chimeras.

Infections and injections

Influenza A/Puerto Rico/8/34 (A/PR/8, H1N1) was grown and harvested as previously described (Doucett et al., 2005). Mice were anesthetized with isoflurane and infected with a previously titrated dose of the virus in 40 μl PBS.

For passive protection experiments, serum was collected from the control and PRDM-$1^{\Delta Ex1A}$ mice and IgM concentrations determined by ELISA. Serum containing 25 μg of IgM diluted in PBS (200 μl total volume) was injected into the lateral tail vein of groups of B cell–deficient μMT mice 2 h before influenza infection.

qRT-PCR

For viral load measurements, whole lungs were collected 24 h after infection with Influenza A/PR/8 and placed into an M

tube (Miltenyi Biotec) on ice containing 1 µl of PBS. Lungs were processed using a gentleMACS dissociator (Miltenyi Biotec) until homogenized. Samples were centrifuged for 5 min at 600 g, and supernatants were frozen at –80°C.

Viral RNA was isolated from lung supernatant using a QIAamp Viral RNA Mini kit (QIAGEN) per the manufacturer's instructions. cDNA was generated using random hexamer primers (Invitrogen) and SuperScript II reverse transcription (Invitrogen). qRT-PCR was performed using Influenza A primers AM-151/AM-397 and probe AM-245 (Schweiger et al., 2000).

For gene expression, mRNA was isolated from cells using an RNeasy mini kit (QIAGEN) per the manufacturer's instructions. cDNA was generated as previously described. For *prdm1* expression in Fig. 5 F, qRT-PCR was performed on a 7900HT Fast Real-Time PCR system (Applied Biosystems) using Sybr Green Master Mix (Thermo Fisher Scientific) and primers for *gapdh* (F: 5′-ACGGCCGCATCT TCTTGTGCA-3′; R: 5′-AATGGCAGCCCTGGTGAC CA-3′) and *prdm1* (F: exon 5, 5′-GGCTCCACTACCCTT ATCCTG-3′; R: exon 6, 5′-TCCTTTTGGAGGGATTGG AGTC-3′). In Fig. 6 C, qRT-PCR was performed using commercially available TaqMan primer/probe mixes (Thermo Fisher Scientific) for *prdm1*, *irf4*, *zbtb20*, *igj*, and *ubc*. For *igj* expression in follicular B cells, only one of three samples gave a positive signal. To allow for graphical representation of Ct(gene)–Ct(*ubc*), the two negative samples were given the maximum Ct value of 40.

Flow cytometry

Single-cell suspensions from tissues were obtained by grinding tissues between the frosted ends of two glass slides and were stained as described previously (Rothaeusler and Baumgarth, 2006). BM cells were obtained from the tibia, fibula, and humerus by flushing the bones with "staining media" (Rothaeusler and Baumgarth, 2006) using a 27-g needle. Peritoneal cavity washout was collected by injecting the peritoneal cavity with staining media using glass Pasteur pipettes and a bulb, agitating the cavity, and extracting the fluid. Single-cell suspensions were treated with ACK lysis buffer (Rothaeusler and Baumgarth, 2006) to lyse red blood cells. Fc receptors were blocked with anti-CD16/32 antibody (2.4G2), and cells were stained on ice with the following fluorochrome conjugates: CD19–Cy5PE (clone ID3), CD4 (GK1.5)–, CD8a (53-6.7)–, CD90.2 (30H12.1)–, F4/80 (F4/80)–, Gr-1 (RB68C5)–, and NK1.1 (PK136)–Pacific blue, IgM (331)–Cy7-allophycocyanin, allophycocyanin, FITC, biotin, IgM^a (DS-1.1)-allophycocyanin, IgM^b (AF6-78.2.5)-allophycocyanin, IgD (11-26)-Cy7PE, IgD^a (AMS-9.1.1)-Cy7PE, IgD^b (AF6-122)-Cy7PE, CD138 (281-2)-allophycocyanin, CD45.1 (A20)-FITC, CD43 (S7)-PE, APC, Pacific blue, CD5 (53-7.8)-biotin, PE, CD23 (B3B4.2)-FITC, biotin, BP1 (6C3-6)-FITC, B220 (RA3-6B2)-Cy7APC, FITC (all generated in-house); IgG3-biotin (BD, R40-82), CD138-BV605 (BD), CD21-BV605 (BD), CD45R-efluor780 (eBioscience), CD19-BV786 (BD), CD93-PE (BD), CD24-BV711 (BD), Streptavidin–Qdot 605 (Thermo Fisher Scientific), and Streptavidin-allophycocyanin (eBioscience). Dead cells were identified using Live/Dead Fixable Violet or Live/Dead Fixable Aqua stain (Invitrogen). FACS analysis was done using a 4-laser, 22-parameter LSR Fortessa (BD). Cells were sorted using a three-laser FACSAria (BD) as described by Rothaeusler and Baumgarth (2006). A 100-µm nozzle was used for sorting, and pressure was set to 18 psi. Data were analyzed using FlowJo software (FlowJo LLC; provided by A. Treister, Treestar Inc., Ashland, OR).

BrdU incorporation

BrdU staining was performed as described previously (Rothaeusler and Baumgarth, 2006). For B-1a, B-1b, and B-1PC turnover rates, mice were injected i.p. for 2 d with BrdU (BD). Overall percent BrdU incorporation was determined in each population, and percentages were divided by 2 to determine turnover per day. Spleen and BM cells were stained for surface markers as described previously. Cells were fixed for 30 min on ice with Cytoperm/Cytofix (BD) and were frozen overnight at –80°C in 90% FBS/10% DMSO. Cells were thawed within 7 d, refixed with Cytoperm/Cytofix, and treated for 1 h with 25 U/6.25 × 10^6 cells of DNase I at 37°C (Worthington Biochemical Corporation). Cells were then stained at room temperature with anti–BrdU-FITC (BD).

Fluorescent microscopy

Spleen and BM cells from Blimp-1 reporter mice and C57BL/6 mice were stained as described above with CD19-Cy5PE (clone ID3), CD4 (GK1.5)–, CD8a (53-6.7)–, F4/80 (F4/80)–, Gr-1 (RB68C5)–, and NK1.1 (PK136)–Pacific blue, IgM (331)-PE, IgD (11-26)-Cy7PE, and CD43 (S7)-allophycocyanin (for reporter mice) or CD138 (281-2)-allophycocyanin (for C57BL/6 mice). Cells were then fixed with Cytofix/Cytoperm and stained intracellularly with anti–GFP-FITC (Abcam) and IgM (331)–Alexa Fluor 594. B-1 cells ($Dump^{neg}CD19^+IgM^{hi}IgD^{lo}CD43^+YFP^{neg}$) and B-1PC ($Dump^{neg}CD19^{neg}IgM^{hi}IgD^{lo}CD43^+YFP^+$) cells were sorted as described above from Blimp-1 YFP mice. In C57BL/6 mice, $Dump^{neg}CD19^{neg}IgM^{hi}IgD^{lo}CD138^+$ and $Dump^{neg}CD19^+IgM^{hi}IgD^{lo}CD138^{neg}$ cells were sorted as non–YFP-expressing controls for B-1PC and B-1–like cells.

Cytospin preparations were made for each sorted population, and cells were mounted using Merifluor Mounting Medium (Meridian Diagnostics). Images were collected on an Olympus BX61 microscope with an Olympus DP72 color camera and were processed with ImageJ (National Institutes of Health) software.

Magnetic cell purification

For experiments culturing peritoneal cavity B cells, autoMACS (Miltenyi Biotec) was used to purify $CD19^+$ cells. Cells were labeled with CD19-biotin, then with anti-biotin magnetic microbeads (Miltenyi Biotec). Purities were >95% as determined by flow cytometry.

To purify peritoneal cavity B-1 cells, autoMACS depletion was used. Cells were labeled and run on autoMACS as above, with biotinylated CD4, CD8a, Gr-1, F4/80, and NK1.1. The negative fraction was washed into PBS for injection. Purity was >90% as determined by flow cytometry.

Tissue cultures

For measurement of *prdm1* expression and secreted IgM in culture supernatant, 2.5×10^5 live cells/well counted using a hemocytometer and Trypan blue were plated into 96-well U bottom tissue culture plates (BD). If indicated, LPS was added at 10 µg/ml. Cells were incubated for 3 d at 37°C/5% CO_2. Supernatants were collected and stored at −20°C until use. Cells were immediately processed for mRNA.

ELISPOTs

IgM ASCs were enumerated as described previously (Doucett et al., 2005). In brief, anti-IgM (331) or anti-IgG3 (SouthernBiotech) was coated overnight onto 96-well plates (Multi-Screen HA Filtration, EMD Millipore). Plates were blocked with PBS/4% BSA. Live cells counted using Trypan blue exclusion were either serially diluted twofold into the ELISPOT plate in culture media (RPMI 1640 [Gibco], 10% heat-inactivated fetal bovine serum, 292 µg/ml L-glutamine, 100 units/ml penicillin, 100 µg/ml streptomycin, 50 µM 2-mercaptoethanol) or were directly deposited by FACS into culture media–containing wells. Plates were incubated overnight at 37°C/5% CO_2. IgM binding was identified with biotinylated anti-IgM (SouthernBiotech), biotinylated anti-IgM^a (BD), biotinylated anti-IgM^b (BD), or biotinylated anti-IgG3 (SouthernBiotech), followed by Streptavidin–Horseradish Peroxidase (Vector Laboratories) and the substrate 3-amino-9-ethylcarbazole (Sigma-Aldrich). Spots were enumerated, and spot sizes, expressed as the number of pixels, were determined using the AID EliSpot Reader System (Autoimmun Diagnostika). Total BM spots were calculated based on the assumption that one femur = 12.7% of total BM cells (Benner et al., 1981).

ELISA

Sandwich ELISAs were performed as previously described (Rothaeusler and Baumgarth, 2006). In brief, 96 well plates were coated with isotype-specific anti-Ig (SouthernBiotech). Nonspecific binding was blocked with blocking buffer (PBS, 1% heat-inactivated NCS, 0.1% dried milk powder, 0.05% Tween20). Twofold serial dilutions in PBS of Ig isotype standards (SouthernBiotech), IgM^a (purified from Igha C57BL/6 mice), IgM^b (CBPC112), serum samples, and culture supernatants were added to the plate at previously determined optimal predilutions. Binding was revealed using isotype-specific biotinylated anti-Ig (SouthernBiotech), anti-IgM^a, or anti-IgM^b (BD), followed by Streptavadin–Horseradish Peroxidase (Vector Laboratories), all diluted in blocking buffer. Plates were developed with 0.005% 3,3′, 5,5′-tetramethylbenzidine (TMB) in 0.05 M of citric acid with 0.015% hydrogen peroxide, and the reaction was stopped with 1 N of sulfuric acid. Absorbance was measured at wavelengths of 450 nm, with reference wavelengths of 595 nm using the SpectraMax M5 (Molecular Devices). Antibody concentrations were determined by comparing them to the standards.

Statistical analysis

Statistical analysis was done using a two-tailed Student's *t* test with the help of Prism software (GraphPad Software). $P < 0.05$ was considered statistically significant.

ACKNOWLEDGMENTS

The authors would like to thank Abigail Spinner and Frank Ventimiglia (California National Primate Research Center, Davis, CA) for their help with flow cytometry and fluorescent microscopy, respectively; Dr. M. Nussenzweig for the Blimp-1 YFP mice; Drs. E. Bikoff and M. Morgan (University of Oxford, Oxford, England, UK) for the PRDM-$1^{\Delta Ex1A}$ mice and PCR protocols; Drs. A. Bäumler and F. Faber (University of California, Davis, Davis, CA) for the germ-free mice; and Drs. E. Meffre (Yale University, New Haven, CT) and Martin Flajnik (University of Maryland, College Park, MD) for advice and discussions.

The project described was supported in part by National Institutes of Health (NIH) grants NIH/NIAID R01AI051354, R01AI085568, and U19AI109962 and the National Center for Advancing Translational Sciences at the NIH through grant number UL1 TR000002 and linked award TL1 TR000133, 2T32OD010931-09, 5T35OD010956-14, and T-32 AI060555.

The authors declare no competing financial interests.

Author contributions: H.P. Savage and N. Baumgarth conceived experiments and analyzed data. H.P. Savage, V.M. Yenson, S.J. Sawhney, and B.J. Mousseau conducted experiments. F.E. Lund provided reagents; H.P. Savage and N. Baumgarth wrote the manuscript. All authors provided manuscript edits.

Submitted: 18 July 2016

Revised: 27 April 2017

Accepted: 8 June 2017

REFERENCES

Alugupalli, K.R., R.M. Gerstein, J. Chen, E. Szomolanyi-Tsuda, R.T. Woodland, and J.M. Leong. 2003. The resolution of relapsing fever borreliosis requires IgM and is concurrent with expansion of B1b lymphocytes. *J. Immunol.* 170:3819–3827. http://dx.doi.org/10.4049/jimmunol.170.7.3819

Baumgarth, N., O.C. Herman, G.C. Jager, L. Brown, L.A. Herzenberg, and L.A. Herzenberg. 1999. Innate and acquired humoral immunities to influenza virus are mediated by distinct arms of the immune system. *Proc. Natl. Acad. Sci. USA.* 96:2250–2255. http://dx.doi.org/10.1073/pnas.96.5.2250

Baumgarth, N., O.C. Herman, G.C. Jager, L.E. Brown, L.A. Herzenberg, and J. Chen. 2000. B-1 and B-2 cell–derived immunoglobulin M antibodies are nonredundant components of the protective response to influenza virus infection. *J. Exp. Med.* 192:271–280. http://dx.doi.org/10.1084/jem.192.2.271

Benner, R., A.V. Oudenaren, and G. Koch. 1981. Induction of antibody formation in mouse BM. *In* Immunological Methods. L. Lefkovits and B. Pernis, editors. Academic Press, New York. 247–261. http://dx.doi.org/10.1016/B978-0-12-442702-0.50020-0

Boes, M., A.P. Prodeus, T. Schmidt, M.C. Carroll, and J. Chen. 1998. A critical role of natural immunoglobulin M in immediate defense against systemic bacterial infection. *J. Exp. Med.* 188:2381–2386. http://dx.doi.org/10.1084/jem.188.12.2381

Boes, M., T. Schmidt, K. Linkemann, B.C. Beaudette, A. Marshak-Rothstein, and J. Chen. 2000. Accelerated development of IgG autoantibodies and autoimmune disease in the absence of secreted IgM. *Proc. Natl. Acad. Sci. USA.* 97:1184–1189. http://dx.doi.org/10.1073/pnas.97.3.1184

Bos, N.A., C.G. Meeuwsen, B.S. Wostmann, J.R. Pleasants, and R. Benner. 1988. The influence of exogenous antigenic stimulation on the specificity repertoire of background immunoglobulin-secreting cells of different isotypes. *Cell. Immunol.* 112:371–380. http://dx.doi.org/10.1016/0008-8749(88)90306-1

Bos, N.A., H. Kimura, C.G. Meeuwsen, H. De Visser, M.P. Hazenberg, B.S. Wostmann, J.R. Pleasants, R. Benner, and D.M. Marcus. 1989. Serum immunoglobulin levels and naturally occurring antibodies against carbohydrate antigens in germ-free BALB/c mice fed chemically defined ultrafiltered diet. *Eur. J. Immunol.* 19:2335–2339. http://dx.doi.org/10.1002/eji.1830191223

Castro, C.D., Y. Ohta, H. Dooley, and M.F. Flajnik. 2013. Noncoordinate expression of J-chain and Blimp-1 define nurse shark plasma cell populations during ontogeny. *Eur. J. Immunol.* 43:3061–3075. http://dx.doi.org/10.1002/eji.201343416

Chevrier, S., D. Emslie, W. Shi, T. Kratina, C. Wellard, A. Karnowski, E. Erikci, G.K. Smyth, K. Chowdhury, D. Tarlinton, and L.M. Corcoran. 2014. The BTB-ZF transcription factor Zbtb20 is driven by Irf4 to promote plasma cell differentiation and longevity. *J. Exp. Med.* 211:827–840. http://dx.doi.org/10.1084/jem.20131831

Choi, Y.S., and N. Baumgarth. 2008. Dual role for B-1a cells in immunity to influenza virus infection. *J. Exp. Med.* 205:3053–3064. http://dx.doi.org/10.1084/jem.20080979

Choi, Y.S., J.A. Dieter, K. Rothaeusler, Z. Luo, and N. Baumgarth. 2012. B-1 cells in the bone marrow are a significant source of natural IgM. *Eur. J. Immunol.* 42:120–129. http://dx.doi.org/10.1002/eji.201141890

Colombo, M.J., G. Sun, and K.R. Alugupalli. 2010. T-cell-independent immune responses do not require CXC ligand 13-mediated B1 cell migration. *Infect. Immun.* 78:3950–3956. http://dx.doi.org/10.1128/IAI.00371-10

Doucett, V.P., W. Gerhard, K. Owler, D. Curry, L. Brown, and N. Baumgarth. 2005. Enumeration and characterization of virus-specific B cells by multicolor flow cytometry. *J. Immunol. Methods.* 303:40–52. http://dx.doi.org/10.1016/j.jim.2005.05.014

Düber, S., M. Hafner, M. Krey, S. Lienenklaus, B. Roy, E. Hobeika, M. Reth, T. Buch, A. Waisman, K. Kretschmer, and S. Weiss. 2009. Induction of B-cell development in adult mice reveals the ability of bone marrow to produce B-1a cells. *Blood.* 114:4960–4967. http://dx.doi.org/10.1182/blood-2009-04-218156

Ehrenstein, M.R., H.T. Cook, and M.S. Neuberger. 2000. Deficiency in serum immunoglobulin (Ig)M predisposes to development of IgG autoantibodies. *J. Exp. Med.* 191:1253–1258. http://dx.doi.org/10.1084/jem.191.7.1253

Engel, P., L.-J. Zhou, D.C. Ord, S. Sato, B. Koller, and T.F. Tedder. 1995. Abnormal B lymphocyte development, activation, and differentiation in mice that lack or overexpress the CD19 signal transduction molecule. *Immunity.* 3:39–50. http://dx.doi.org/10.1016/1074-7613(95)90157-4

Esplin, B.L., R.S. Welner, Q. Zhang, L.A. Borghesi, and P.W. Kincade. 2009. A differentiation pathway for B1 cells in adult bone marrow. *Proc. Natl. Acad. Sci. USA.* 106:5773–5778. http://dx.doi.org/10.1073/pnas.0811632106

Fairfax, K.A., L.M. Corcoran, C. Pridans, N.D. Huntington, A. Kallies, S.L. Nutt, and D.M. Tarlinton. 2007. Different kinetics of blimp-1 induction in B cell subsets revealed by reporter gene. *J. Immunol.* 178:4104–4111. http://dx.doi.org/10.4049/jimmunol.178.7.4104

Flajnik, M.F. 2002. Comparative analyses of immunoglobulin genes: Surprises and portents. *Nat. Rev. Immunol.* 2:688–698. http://dx.doi.org/10.1038/nri889

Fooksman, D.R., T.A. Schwickert, G.D. Victora, M.L. Dustin, M.C. Nussenzweig, and D. Skokos. 2010. Development and migration of plasma cells in the mouse lymph node. *Immunity.* 33:118–127. http://dx.doi.org/10.1016/j.immuni.2010.06.015

Gavin, A.L., N. Barnes, H.M. Dijstelbloem, and P.M. Hogarth. 1998. Identification of the mouse IgG3 receptor: Implications for antibody effector function at the interface between innate and adaptive immunity. *J. Immunol.* 160:20–23.

Ghosn, E.E., R. Yamamoto, S. Hamanaka, Y. Yang, L.A. Herzenberg, H. Nakauchi, and L.A. Herzenberg. 2012. Distinct B-cell lineage commitment distinguishes adult bone marrow hematopoietic stem cells. *Proc. Natl. Acad. Sci. USA.* 109:5394–5398. http://dx.doi.org/10.1073/pnas.1121632109

Gil-Cruz, C., S. Bobat, J.L. Marshall, R.A. Kingsley, E.A. Ross, I.R. Henderson, D.L. Leyton, R.E. Coughlan, M. Khan, K.T. Jensen, et al. 2009. The porin OmpD from nontyphoidal *Salmonella* is a key target for a protective B1b cell antibody response. *Proc. Natl. Acad. Sci. USA.* 106:9803–9808. http://dx.doi.org/10.1073/pnas.0812431106

Godin, I.E., J.A. Garcia-Porrero, A. Coutinho, F. Dieterlen-Lièvre, and M.A. Marcos. 1993. Para-aortic splanchnopleura from early mouse embryos contains B1a cell progenitors. *Nature.* 364:67–70. http://dx.doi.org/10.1038/364067a0

Haas, K.M., J.C. Poe, D.A. Steeber, and T.F. Tedder. 2005. B-1a and B-1b cells exhibit distinct developmental requirements and have unique functional roles in innate and adaptive immunity to *S. pneumoniae*. *Immunity.* 23:7–18. http://dx.doi.org/10.1016/j.immuni.2005.04.011

Hardy, R.R., and K. Hayakawa. 2001. B cell development pathways. *Annu. Rev. Immunol.* 19:595–621. http://dx.doi.org/10.1146/annurev.immunol.19.1.595

Haury, M., A. Sundblad, A. Grandien, C. Barreau, A. Coutinho, and A. Nobrega. 1997. The repertoire of serum IgM in normal mice is largely independent of external antigenic contact. *Eur. J. Immunol.* 27:1557–1563. http://dx.doi.org/10.1002/eji.1830270635

Hayakawa, K., M. Asano, S.A. Shinton, M. Gui, D. Allman, C.L. Stewart, J. Silver, and R.R. Hardy. 1999. Positive selection of natural autoreactive B cells. *Science.* 285:113–116. http://dx.doi.org/10.1126/science.285.5424.113

Herzenberg, L.A., A.M. Stall, P.A. Lalor, C. Sidman, W.A. Moore, D.R. Parks, and L.A. Herzenberg. 1986. The Ly-1 B cell lineage. *Immunol. Rev.* 93:81–102. http://dx.doi.org/10.1111/j.1600-065X.1986.tb01503.x

Holodick, N.E., K. Repetny, X. Zhong, and T.L. Rothstein. 2009. Adult BM generates CD5+ B1 cells containing abundant N-region additions. *Eur. J. Immunol.* 39:2383–2394. http://dx.doi.org/10.1002/eji.200838920

Holodick, N.E., J.R. Tumang, and T.L. Rothstein. 2010. Immunoglobulin secretion by B1 cells: Differential intensity and IRF4-dependence of spontaneous IgM secretion by peritoneal and splenic B1 cells. *Eur. J. Immunol.* 40:3007–3016. http://dx.doi.org/10.1002/eji.201040545

Holodick, N.E., T. Vizconde, and T.L. Rothstein. 2014. Splenic B-1a cells expressing CD138 spontaneously secrete large amounts of immunoglobulin in naïve mice. *Front. Immunol.* 5:129. http://dx.doi.org/10.3389/fimmu.2014.00129

Honda, S., N. Kurita, A. Miyamoto, Y. Cho, K. Usui, K. Takeshita, S. Takahashi, T. Yasui, H. Kikutani, T. Kinoshita, et al. 2009. Enhanced humoral immune responses against T-independent antigens in Fcα/μR-deficient mice. *Proc. Natl. Acad. Sci. USA.* 106:11230–11235. http://dx.doi.org/10.1073/pnas.0809917106

Ichikawa, D., M. Asano, S.A. Shinton, J. Brill-Dashoff, A.M. Formica, A. Velcich, R.R. Hardy, and K. Hayakawa. 2015. Natural anti-intestinal goblet cell autoantibody production from marginal zone B cells. *J. Immunol.* 194:606–614. http://dx.doi.org/10.4049/jimmunol.1402383

Kallies, A., J. Hasbold, K. Fairfax, C. Pridans, D. Emslie, B.S. McKenzie, A.M. Lew, L.M. Corcoran, P.D. Hodgkin, D.M. Tarlinton, and S.L. Nutt. 2007. Initiation of plasma-cell differentiation is independent of the

transcription factor Blimp-1. *Immunity.* 26:555–566. http://dx.doi.org/10.1016/j.immuni.2007.04.007

Kantor, A.B., A.M. Stall, S. Adams, L.A. Herzenberg, and L.A. Herzenberg. 1992. Differential development of progenitor activity for three B-cell lineages. *Proc. Natl. Acad. Sci. USA.* 89:3320–3324. http://dx.doi.org/10.1073/pnas.89.8.3320

Keim, C., D. Kazadi, G. Rothschild, and U. Basu. 2013. Regulation of AID, the B-cell genome mutator. *Genes Dev.* 27:1–17. http://dx.doi.org/10.1101/gad.200014.112

Khan, W.N., P. Sideras, F.S. Rosen, and F.W. Alt. 1995. The role of Bruton's tyrosine kinase in B-cell development and function in mice and man. *Ann. N.Y. Acad. Sci.* 764:27–38. http://dx.doi.org/10.1111/j.1749-6632.1995.tb55802.x

Kobayashi, M., W.C. Shelley, W. Seo, S. Vemula, Y. Lin, Y. Liu, R. Kapur, I. Taniuchi, and M. Yoshimoto. 2014. Functional B-1 progenitor cells are present in the hematopoietic stem cell-deficient embryo and depend on *Cbfβ* for their development. *Proc. Natl. Acad. Sci. USA.* 111:12151–12156. http://dx.doi.org/10.1073/pnas.1407370111

Koch, M.A., G.L. Reiner, K.A. Lugo, L.S. Kreuk, A.G. Stanbery, E. Ansaldo, T.D. Seher, W.B. Ludington, and G.M. Barton. 2016. Maternal IgG and IgA antibodies dampen mucosal T helper cell responses in early life. *Cell.* 165:827–841. http://dx.doi.org/10.1016/j.cell.2016.04.055

Lalor, P.A., L.A. Herzenberg, S. Adams, and A.M. Stall. 1989. Feedback regulation of murine Ly-1 B cell development. *Eur. J. Immunol.* 19:507–513. http://dx.doi.org/10.1002/eji.1830190315

Mongini, P.K., K.E. Stein, and W.E. Paul. 1981. T cell regulation of IgG subclass antibody production in response to T-independent antigens. *J. Exp. Med.* 153:1–12. http://dx.doi.org/10.1084/jem.153.1.1

Montecino-Rodriguez, E., and K. Dorshkind. 2012. B-1 B cell development in the fetus and adult. *Immunity.* 36:13–21. http://dx.doi.org/10.1016/j.immuni.2011.11.017

Morgan, M.A., E. Magnusdottir, T.C. Kuo, C. Tunyaplin, J. Harper, S.J. Arnold, K. Calame, E.J. Robertson, and E.K. Bikoff. 2009. Blimp-1/Prdm1 alternative promoter usage during mouse development and plasma cell differentiation. *Mol. Cell. Biol.* 29:5813–5827. http://dx.doi.org/10.1128/MCB.00670-09

Muramatsu, M., K. Kinoshita, S. Fagarasan, S. Yamada, Y. Shinkai, and T. Honjo. 2000. Class switch recombination and hypermutation require activation-induced cytidine deaminase (AID), a potential RNA editing enzyme. *Cell.* 102:553–563. http://dx.doi.org/10.1016/S0092-8674(00)00078-7

Nguyen, T.T., R.A. Elsner, and N. Baumgarth. 2015. Natural IgM prevents autoimmunity by enforcing B cell central tolerance induction. *J. Immunol.* 194:1489–1502. http://dx.doi.org/10.4049/jimmunol.1401880

Notley, C.A., M.A. Brown, G.P. Wright, and M.R. Ehrenstein. 2011. Natural IgM is required for suppression of inflammatory arthritis by apoptotic cells. *J. Immunol.* 186:4967–4972. http://dx.doi.org/10.4049/jimmunol.1003021

Nutt, S.L., P.D. Hodgkin, D.M. Tarlinton, and L.M. Corcoran. 2015. The generation of antibody-secreting plasma cells. *Nat. Rev. Immunol.* 15:160–171. http://dx.doi.org/10.1038/nri3795

Ochsenbein, A.F., T. Fehr, C. Lutz, M. Suter, F. Brombacher, H. Hengartner, and R.M. Zinkernagel. 1999. Control of early viral and bacterial distribution and disease by natural antibodies. *Science.* 286:2156–2159. http://dx.doi.org/10.1126/science.286.5447.2156

Ohdan, H., K.G. Swenson, H.S. Kruger Gray, Y.G. Yang, Y. Xu, A.D. Thall, and M. Sykes. 2000. Mac-1-negative B-1b phenotype of natural antibody-producing cells, including those responding to Gal α 1,3Gal epitopes in α 1,3-galactosyltransferase-deficient mice. *J. Immunol.* 165:5518–5529. http://dx.doi.org/10.4049/jimmunol.165.10.5518

Perlmutter, R.M., D. Hansburg, D.E. Briles, R.A. Nicolotti, and J.M. Davie. 1978. Subclass restriction of murine anti-carbohydrate antibodies. *J. Immunol.* 121:566–572.

Reynolds, A.E., M. Kuraoka, and G. Kelsoe. 2015. Natural IgM is produced by CD5$^-$ plasma cells that occupy a distinct survival niche in bone marrow. *J. Immunol.* 194:231–242. http://dx.doi.org/10.4049/jimmunol.1401203

Rickert, R.C., K. Rajewsky, and J. Roes. 1995. Impairment of T-cell-dependent B-cell responses and B-1 cell development in CD19-deficient mice. *Nature.* 376:352–355. http://dx.doi.org/10.1038/376352a0

Rothaeusler, K., and N. Baumgarth. 2006. Evaluation of intranuclear BrdU detection procedures for use in multicolor flow cytometry. *Cytometry A.* 69A:249–259. http://dx.doi.org/10.1002/cyto.a.20252

Rutishauser, R.L., G.A. Martins, S. Kalachikov, A. Chandele, I.A. Parish, E. Meffre, J. Jacob, K. Calame, and S.M. Kaech. 2009. Transcriptional repressor Blimp-1 promotes CD8(+) T cell terminal differentiation and represses the acquisition of central memory T cell properties. *Immunity.* 31:296–308. http://dx.doi.org/10.1016/j.immuni.2009.05.014

Savitsky, D., and K. Calame. 2006. B-1 B lymphocytes require Blimp-1 for immunoglobulin secretion. *J. Exp. Med.* 203:2305–2314. http://dx.doi.org/10.1084/jem.20060411

Schweiger, B., I. Zadow, R. Heckler, H. Timm, and G. Pauli. 2000. Application of a fluorogenic PCR assay for typing and subtyping of influenza viruses in respiratory samples. *J. Clin. Microbiol.* 38:1552–1558.

Shapiro-Shelef, M., K.I. Lin, L.J. McHeyzer-Williams, J. Liao, M.G. McHeyzer-Williams, and K. Calame. 2003. Blimp-1 is required for the formation of immunoglobulin secreting plasma cells and pre-plasma memory B cells. *Immunity.* 19:607–620. http://dx.doi.org/10.1016/S1074-7613(03)00267-X

Solvason, N., A. Lehuen, and J.F. Kearney. 1991. An embryonic source of Ly1 but not conventional B cells. *Int. Immunol.* 3:543–550. http://dx.doi.org/10.1093/intimm/3.6.543

Tumang, J.R., R. Francés, S.G. Yeo, and T.L. Rothstein. 2005. Spontaneously Ig-secreting B-1 cells violate the accepted paradigm for expression of differentiation-associated transcription factors. *J. Immunol.* 174:3173–3177. http://dx.doi.org/10.4049/jimmunol.174.6.3173

van Furth, R., H.R. Schuit, and W. Hijmans. 1965. The immunological development of the human fetus. *J. Exp. Med.* 122:1173–1188. http://dx.doi.org/10.1084/jem.122.6.1173

Van Oudenaren, A., J.J. Haaijman, and R. Benner. 1984. Frequencies of background cytoplasmic Ig-containing cells in various lymphoid organs of athymic and euthymic mice as a function of age and immune status. *Immunology.* 51:735–742.

Watanabe, N., K. Ikuta, S. Fagarasan, S. Yazumi, T. Chiba, and T. Honjo. 2000. Migration and differentiation of autoreactive B-1 cells induced by activated γ/δ T cells in antierythrocyte immunoglobulin transgenic mice. *J. Exp. Med.* 192:1577–1586. http://dx.doi.org/10.1084/jem.192.11.1577